Environmental Science and Pollution Research (2023) 30:79026–79048
https://doi.org/10.1007/s11356-023-28102-x

RESEARCH ARTICLE

Effect of capping mode on control of phosphorus release from sediment by lanthanum hydroxide

Fujun Sun[1] · Yanhui Zhan[1] · Jianwei Lin[1]

Received: 20 March 2023 / Accepted: 31 May 2023 / Published online: 6 June 2023

Abstract

The use of in situ active capping to control phosphorus release from sediment has attracted more and more attentions in recent years. It is important to identify the effect of capping mode on the control of phosphorus release from sediment by the in situ active capping method. In this study, the impact of capping mode on the restraint of phosphorus migration from sediment into overlying water (OW) by lanthanum hydroxide (LH) was studied. Under no suspended particulate matter (SPM) deposition condition, LH capping effectively restrained the liberation of endogenous phosphorus into OW during anoxia, and the inactivation of diffusive gradient in thin film-unstable phosphorus (UP_{DGT}) and mobile phosphorus (P_{Mobile}) in the topmost sediment served as a significant role in the restraint of endogenous phosphorus migration into OW by LH capping. Under no SPM deposition, although the transformation of capping mode from the single high dose capping to the multiple smaller doses capping had a certain negative impact on the restraint efficiency of endogenous phosphorus liberation to OW by LH in the early period of application, it increased the stability of phosphorus in the static layer in the later period of application. Under SPM deposition condition, LH capping had the capability to mitigate the risk of endogenous phosphorus liberation into OW under anoxia conditions, and the inactivation of UP_{DGT} and P_{Mobile} in the topmost sediment was a significant mechanism for the control of sediment phosphorus liberation into OW by LH capping. Under SPM deposition condition, the change in the covering mode from the one-time high dose covering to the multiple smaller doses covering decreased the efficiency of LH to limit the endogenous phosphorus transport into OW in the early period of application, but it increased the performance of LH to restrain the sedimentary P liberation during the later period of application. The results of this work suggest that the multiple LH capping is a promising approach for controlling the internal phosphorus loading in freshwater bodies where SPM deposition often occurs in the long run.

Keywords Lanthanum hydroxide · One-time capping · Multiple capping · Sediment · Phosphorus · Capping mode

Introduction

Eutrophication of surface water bodies is a severe environmental issue globally (Balasuriya et al. 2022; Sun et al. 2022; Zhou et al. 2022). The occurrence of eutrophication in water bodies not only can cause the harmful algal blooms, bottom water hypoxia, water quality deterioration, biodiversity loss, and ecosystem degradation but also can give rise to the disruption of drinking water supplies and the closure of commercial fisheries (Feng et al. 2023; Le Moal et al. 2019; Mackay et al. 2022; Rozemeijer et al. 2021). A lot of researchers have found that phosphorus (P) is a key limiting factor causing eutrophication in freshwater bodies (Determan et al. 2021; Schindler 1977; Schindler et al. 2016). As such, the reduction in the phosphorus loading is critical to the control of eutrophication in freshwater bodies (Carpenter 2008; Yu et al. 2022). The sources of phosphorus in surface waters could be divided into two categories, namely, external phosphorus source (such as wastewater discharge and runoff from agriculture) and internal phosphorus source (phosphorus released from sediments) (Smith et al. 1999; Wen et al. 2020; Yang et al. 2020a). In order to mitigate the eutrophication of surface water bodies, it is important for reducing the input of exogenous phosphorus (Schindler et al. 2016; Yang et al. 2020a). However, after the input of exogenous phosphorus is controlled, reducing the release of endogenous

Responsible Editor: V.V.S.S. Sarma

✉ Jianwei Lin
jwlin@shou.edu.cn

[1] College of Marine Ecology and Environment, Shanghai Ocean University, Shanghai 201306, China

phosphorus is regarded as the key for combating the eutrophication in surface water bodies (Jeppesen et al. 2005; Sondergaard et al. 2003; Wen et al. 2020; Yang et al. 2020a; Zhang et al. 2023).

Up to now, a series of sediment restoration techniques have been proposed to reduce the internal phosphorus loading, including sediment dredging (Li et al. 2020; Yang et al. 2023; Yin et al. 2021), chemical phosphorus inactivation using aluminum salt (Huang et al. 2016; Huser et al. 2016), sediment oxidation (Yamada et al. 2012), sediment microbial fuel cells (Wang et al. 2022), aquatic plant restoration (Li et al. 2021), aeration (Chen et al. 2021a), electrokinetic isolation (Tang et al. 2020), inert capping (Jiao et al. 2020), and active capping/addition (AC/A) (Chen et al. 2021b; Hong et al. 2022; Wu et al. 2022a). Among these technologies, AC/A, which involves the placement of P-inactivation sorbent materials (PISMs) on the interface of overlying water (OW) and sediment or the amendment of sediments with PISMs, shows great potential in the restraint of internal phosphorus release to OW (Fan et al. 2017; Lei et al. 2022; Li et al. 2023; Xia et al. 2023). A lot of metal-based PISMs have been utilized to address the problem of endogenous phosphorus release into OW, including iron-based PISMs (Fuchs et al. 2018; Wang et al. 2021a; Zhan et al. 2019), aluminum-based PISMs (Li et al. 2017; Wang et al. 2019; Yin et al. 2018b), calcium-based PISMs (Yin et al. 2016; Zhou et al. 2019), zirconium-based PISMs (Lin et al. 2019b, 2020b), and lanthanum-based PISMs (Lin et al. 2019d; Wu et al. 2022a; Zeller & Alperin 2021). Among them, lanthanum-based PISM (La-PISM) is considered a highly promising material for the immobilization of phosphorus in sediment and the restraint of sediment internal phosphorus release into OW because of the strong affinity of lanthanum for phosphate, high selectivity of lanthanum to phosphate, and high stability of $LaPO_4$ (Ding et al. 2018; Fang et al. 2018; He et al. 2022; Li et al. 2019; Meis et al. 2013; Waajen et al. 2016; Wang et al. 2017; Wu et al. 2022a; Yasseri & Epe 2016).

For the AC/A approach, PISMs can be added with a single high dose or added with multiple small doses (Meis et al. 2013; Yin et al. 2018c). Mei et al. found that compared to a single high dose, it is probable that applying PISMs with multiple smaller doses increases the cost-effectiveness and decreases the non-target effects (Meis et al. 2013). Yin et al. observed that under the action of intensive bioturbation, the vertical movement of the applied PISMs in sediment can take place, which increases the potential of P flux across sediment-OW interface (Yin et al. 2018c). In this case, it may be necessary to either remove the sediment biota or repeatedly dose the PISMs into the contaminated sediment (Yin et al. 2018c). Thus, comparing the effectiveness and mechanism of PISMs capping/addition with a single high dose and multiple small doses to mitigate sediment phosphorus release is extremely critical to the application AC/A method to restrain the internal phosphorus release into OW.

Suspended particulate matter (SPM) is widely present in natural aquatic environments (Ho et al. 2022; Walch et al. 2022). The deposition of SPM will inevitably lead to the formation of the new sediment on the old sediment (Liu et al. 2019). After the surface sediment is covered with PISMs, the newly formed sediment due to the SPM deposition will bury the formed capping system (Lei et al. 2021; Liu et al. 2016; Yin et al. 2017). SPM can serve as a source of phosphorus in water because of desorption/release or a sink of phosphorus in water due to adsorption/uptake (Ji et al. 2022; Yang et al. 2020b). Yin et al. observed that the deposition of SPM can bury PISMs deeper into the sediment layer, resulting in the increase in the amount of potentially mobile P (P_{Mobile}) in the surface sediment and the flux of dissolved reactive P (DRP) across the sediment-OW interface (Yin et al. 2018a, 2017). Consequently, comparing the effectiveness and mechanism of PISMs capping and addition with a single high dose and multiple small doses to intercept sedimentary phosphorus release under SPM deposition condition is critical to the utilization of AC/A approach to manage the sediment internal phosphorus loading.

Capping is less laborious PISM application mode than amendment (Abel et al. 2017). Lanthanum hydroxide (LH) is a common lanthanum-based PISM. LH has strong adsorption capability to phosphate even at trace levels ($H_zPO_4^{z-3}$, $z=0$, 1, 2, or 3) in aqueous solution and is receiving increasing attention (Fang et al. 2017; He et al. 2022; Lin et al. 2019d; Wu et al. 2022a). In addition, LH also has good performance for P inactivation in sediment (Lin et al. 2019d; Wu et al. 2022a). Understanding the effect of capping mode (one-time capping and multiple capping) on the control of phosphorus release from sediment by LH in the absence and presence of SPM deposition is vital to the application of LH as an active capping material to block sediment phosphorus release. However, little information is available on the impact of capping mode on the control of internal phosphorus release to OW by LH.

Our work is aimed at studying the impact of capping mode (one-time capping and multiple capping) on the control of sediment phosphorus release into OW by LH in the absence and presence of SPM deposition. To realize this goal, the behavior and mechanism of $H_zPO_4^{z-3}$ adsorption from aqueous solution onto LH were investigated using batch experiments and X-ray photoelectron spectroscopy firstly, and then the influence of one-time and multiple LH capping on the migration of P from sediment to OW in the absence and presence of SPM deposition was comparatively explored using sediment incubation experiments. The results of this work will be conductive to the application of LH to inhibit the endogenous phosphorus release into OW.

Materials and methods

Materials

The sediment and OW used in the present study were sampled from a small scenic surface water body located in Pudong New Area, Shanghai, China. The thoroughly homogenized wet sediment was used to construct the sediment core in the incubation experiment. The air-dried sediment sample with a particle size of less than 0.15 mm was adopted as the SPM in the incubation experiment. All chemicals employed in this work were of analytical grade agents and obtained from Sinopharm Chemical Reagents Co., Ltd., China. The zirconium oxide-Chelex based diffusive gradient in thin film (ZrO-Chelex DGT) was purchased from EasySensor Ltd., China.

Preparation and characterization of LH

Lanthanum hydroxide was prepared by precipitating $LaCl_3$ in NaOH. First, 20 g of $LaCl_3{\cdot}6H_2O$ was added to 100 mL of deionized water (DI-water). Next, the pH of the as-obtained La(III) solution was adjusted to 11 by adding a 1 mol/L sodium hydroxide solution dropwise under agitation condition. Then, stirring was continued for one hour. Subsequently, the reaction precipitate was collected from the suspension solution through centrifugation. Then, the product was washed 5 times with DI-water. In the end, the washed precipitate was air-dried, ground, and passed through the sieve with 100 meshes.

The X-ray diffraction (XRD) spectrum of LH was acquired using a SMARTLAB9 XRD spectrometer (RIKEN Corporation, Japan) with Cu/Kα radiation. The pH drift approach was employed to measure the pH of zero charge point (pH_{PZC}) of LH (Zyoud et al. 2019). Briefly, 10 mg of LH was introduced into 50 mL of 0.01 mol/L sodium nitrate solutions, whose initial pH (pH_i) values were 5, 6, 7, 8, 9, 10, and 11, respectively. After that, the reaction system was shaken at 150 rpm and 298 K. After 24 h of reaction, the final pH (pH_f) was determined by a pH meter. The pH_{PZC} of LH was estimated from the plot of pH_i-pH_f versus pH_i. The Brunauer–Emmett–Teller (BET) specific surface area, mean pore diameter, and total pore volume of LH were determined using a Tristar II 3020 surface area and porosity size analyzer, which was provided by Micromeritics, USA. An Escalab 250Xi X-ray photoelectron spectrometer, which was provided by Thermo Fisher Scientific, USA, was employed to explore the interaction between LH and $H_zPO_4^{z-3}$. The XPSPEAK41 software was employed to fit the XPS spectrum. The Shirley background was used. The ratio of Lorentzian to Gaussian was fixed at 30%.

Adsorption experiment

The influences of reaction time, initial phosphorus concentration, and pH value on the adsorption of $H_zPO_4^{z-3}$ onto LH were investigated by batch experiments. In the adsorption kinetics experiment, 0.01 g of LH was added into 50 mL of 20 mg P/L phosphate solution with an initial pH value of 7, and the reaction time was set at 15, 30, 45, 60, 120, 240 360, 480, 960, and 1440 min, respectively. In the adsorption isotherm experiment, 0.01 g of LH was introduced into 0.05 L of phosphate solution with an initial pH value of 7 for 24 h, and the initial concentration of $H_zPO_4^{z-3}$ was set at 5, 10, 15, 20, 25, 30, and 40 mg P/L, respectively. In the pH effect experiment, 0.01 g of LH was shaken in 0.05 L of phosphate solution with an initial phosphorus concentration of 20 mg/L for 24 h, and the initial pH values were set at 5, 6, 7, 8, 9, 10, and 11, respectively. In all the adsorption experiments, the formed suspension was stirred by a water bath shaker at 150 rpm and 298 K. After the adsorption reaction was finished, the liquid phase was collected by a 0.45 μm filter membrane. The residual concentration of $H_zPO_4^{z-3}$ in the filtrate was analyzed with a spectrophotometer at 700 nm using the ammonium molybdate method. For the pH influence experiment, the final pH was measured by a pH meter. All the $H_zPO_4^{z-3}$ uptake experiments were implemented in duplicate. The quasi-first-order (QFO, Eq. (1)), quasi-second-order (QSO, Eq. (2)), and Elovich (EH, Eq. (4)) kinetic models were adopted for the analysis of experimental kinetics data (Afridi et al. 2019; Yuan et al. 2023).

$$Q_t = Q_e\left(1 - \exp(-k_1 t)\right) \tag{1}$$

$$Q_t = \frac{k_2 Q_e^2 t}{1 + k_2 Q_e t} \tag{2}$$

$$h = k_2 Q_e^2 \tag{3}$$

$$Q_t = \frac{1}{b}\ln(1 + abt) \tag{4}$$

where Q_t (mg P/g) represents the amount of $H_zPO_4^{z-3}$ adsorbed by LH at time t (min); Q_e (mg P/g) represents the quantity of $H_zPO_4^{z-3}$ adsorbed by LH at equilibrium time; k_1 (1/min) and k_2 (g/mg min) indicate the rate constants of the QFO and QSO equations, respectively; a (mg/g min) indicates the initial rate of $H_zPO_4^{z-3}$ adsorption calculated based on the EH kinetic equation; b (g/mg) indicates the constant of EH kinetic equation; h (mg/g min) represents the initial rate of $H_zPO_4^{z-3}$ adsorption calculated based on the QSO kinetic equation.

The Langmuir (Eq. (5)) and Freundlich (Eq. (6)) isothermal equations were employed to match the adsorption data (Afridi et al. 2019; Tran et al. 2017).

$$Q_e = \frac{Q_m K_L C_e}{1 + K_L C_e} \tag{5}$$

$$Q_e = K_F C_e^{1/n} \tag{6}$$

where Q_e indicates the equilibrated $H_zPO_4^{z-3}$ adsorption capacity (mg P/g); C_e indicates the concentration of $H_zPO_4^{z-3}$ in the equilibrated solution (mg P/L); Q_m (mg P/g) represents the $H_zPO_4^{z-3}$ monolayer saturation adsorption capacity; K_L (L/mg) represents the Langmuir equilibrium constant; K_F and $1/n$ indicate the Freundlich equilibrium constants.

Sediment incubation experiment

Twelve Plexiglas cylinders, whose inner diameter was 10 cm and whose height was 30 cm, were applied to investigate the impact of one-time and multiple LH capping on the transport of phosphorus from sediment to OW in the absence and presence of SPM deposition. The height of the sediment core in the Plexiglas cylinder was 10 cm. The twelve cylinders were separated into six groups (Fig. S1), and each group set two parallel. The cylinders that only contain sediment and OW were used as the control group. For the one-time capping group, 10 g of LH was evenly added to the water surface in cylinder at one time, and the added LH settled to the interface between sediment and OW (SWI), forming the LH capping layer on the SWI. For the multiple capping group, 10 g of LH was divided into five equal parts, and 2 g of LH was added to the water surface in cylinder every 15 days. There were two types of control, one-time capping and multiple capping groups. One is the control, one-time capping or multiple capping group without SPM deposition. The other is the control, one-time capping or multiple capping group with SPM deposition. For the SPM deposition groups, 10 g of SPM was added to the water surface every 5 days, and the number for the addition of SPM was set at 13. Before the addition of OW, its dissolved oxygen (DO) concentration was reduced to below 0.5 mg/L using the sulfite oxidation approach (Kim et al. 2003). Rubber stopper and Vaseline were used to seal cylinder. During the period of incubation, the DO, pH, DRP, and dissolved total phosphorus (DTP) of OW were monitored at regular time. The DO and pH of OW were analyzed by DO and pH meters, respectively. The DRP concentration of OW was measured by the ascorbic acid-molybdenum blue colorimetric method (Yang et al. 2023). The DTP concentration of OW was measured by the potassium persulfate digestion-ammonium molybdate spectrophotometry approach (Yang et al. 2023). On the 145th day, the ZrO-Chelex DGT device was slowly inserted into the sediment and placed for twenty-four hours to determine the concentrations of DGT-unstable phosphorus and iron (abbreviated as UP_{DGT} and UF_{DGT}, respectively) in the sediment/OW profile. After retrieval, the ZrO-Chelex DGT device was marked with the SWI position and cleaned using DI-water (Hu et al. 2022). Then, a ceramic knife was used to cut the ZrO-Chelex DGT gel at intervals, and the gel strip was sequentially immersed in 1000 mmol/L nitric acid and 1000 mmol/L sodium hydroxide solutions, respectively (Fan et al. 2021; Hu et al. 2022). The concentrations of P and Fe in the eluate were determined by the molybdenum blue and phenanthroline colorimetric methods, respectively (Fan et al. 2021; Hu et al. 2022). The concentrations of UP_{DGT} and UF_{DGT} (C_{DGT}) were calculated by Eq. (7) (Chen et al. 2016; Hu et al. 2022):

$$C_{DGT} = \frac{M\Delta g}{DAt} \tag{7}$$

where M (μg) represents the mass of accumulated phosphorus or iron over the time of deployment; Δg (mm) indicates the thickness of the material diffusive layer; D (cm^2/s) represents the diffusive coefficient of phosphorus or iron in the diffusive layer; A (cm^2) represents the exposure area of the gel; t (s) represents the time of deployment.

The M value was determined by Eq. (8) (Hu et al. 2022):

$$M = \frac{C_e(V_g + V_e)}{f_e} \tag{8}$$

where C_e (mg/L) indicates the phosphorus or iron concentration in the eluate; V_g (mL) indicates the volume of the gel; V_e (mL) indicates the volume of the eluate; f_e represents the efficiency of elution.

On day 198, the sediment samples were obtained from the sediment layers at depths of 0–1, 1–2, 2–3, 3–6, and 6–10 cm in the control, one-time capping, and multiple capping groups. The sampled sediment was air-dried, ground, and passed through the sieve with 100 meshes. According to the P sequential extraction method described in the previous literatures (Li & Shi 2020; Lin et al. 2019b; Wang et al. 2022), the P fractions of sediments were determined. In this method, five phosphorus fractions can be obtained, and they are loosely immobilized phosphorus (LI-P), readily reductive phosphorus (RR-P), metal oxide-bound phosphorus (OH-SRP), hydrochloric acid-extractable phosphorus (H-P), and residual phosphorus (R-P). The content of mobile phosphorus (P_{Mobile}) in sediment was calculated as the total amount of LI-P and RR-P (Wang et al. 2013). The quantity of total phosphorus (P_{Total}) in sediment was calculated as the total amount of LI-P, RR-P, OH-SRP, H-P, and R-P.

Results and discussion

Characterization of LH

The XRD pattern of LH is displayed in Fig. 1a. The principal XRD peaks of LH were basically identical to those of lanthanum hydroxide crystal (JCPDS 36–1481) (Zhang et al. 2022). This demonstrates that the as-prepared LH sample is primarily composed of lanthanum hydroxide crystal. The pH_{PZC} of LH was found to be 6.12 (Fig. 1b). This indicates that the surface of LH possesses net positive charges at pH below 6.12, but its surface possesses net negative charges at pH above 6.12. The BET surface area of LH was 37.7 m^2/g. The total pore volume of LH was 0.0186 cm^3/g. The mean pore diameter of LH was 2.09 nm.

Adsorption characteristics and mechanism of phosphate on LH

The kinetic curve of $H_zPO_4^{z-3}$ adsorption by LH is displayed in Fig. 2a. From Fig. 2a, we can observe that with the rise of adsorption time from 0 to 960 min, the $H_zPO_4^{z-3}$ adsorption capacity for LH gradually increased. During the early adsorption stage, the $H_zPO_4^{z-3}$ adsorption was quick (Fig. 2a). This was due to the fact that there were a large number of active adsorption sites on the surface of LH in the initial adsorption stage (Zhang et al. 2021). The QFO, QSO, and EH models were adopted for the analysis of experimental kinetics data, and the relevant parameters were obtained as shown in Table 1. The EH kinetic model ($R^2 = 0.988$) described the adsorption process of $H_zPO_4^{z-3}$ onto LH better than the QSO ($R^2 = 0.882$) kinetic model. Furthermore, the QSO kinetic model ($R^2 = 0.882$) described the adsorption process of $H_zPO_4^{z-3}$ onto LH better than the QFO kinetic model ($R^2 = 0.713$). The EH model is widely applied to chemisorption data (Tran et al. 2017). The good fitting of kinetic data to the QSO model generally indicates that the adsorption process mainly obeys a chemisorption process (Asaoka et al. 2021; Luo et al. 2023; Wang et al. 2021b). Consequently, the uptake of $H_zPO_4^{z-3}$ by LH is largely mediated by chemisorption. The initial adsorption rates calculated based on the QSO and EH kinetic models were 1.65 and 7.45 mg/g min, respectively (Table 1). According to Eq. (9), the mean adsorption rate ($\overline{v}$, mg/g min) at 0–15 min was calculated to be 1.58 mg/(g min).

$$\overline{v} = \frac{Q_{t_1} - Q_{t_2}}{t_1 - t_2} \tag{9}$$

where t_1 and t_2 represent the adsorption time (min); Q_{t_1} and Q_{t_2} (mg/g) represent the $H_zPO_4^{z-3}$ adsorption capacities at t_1 and t_1 (min), respectively. Based on the data reported in the previous literature (Ross et al. 2008), the initial rates of $H_zPO_4^{z-3}$ adsorption onto lanthanum ion-modified bentonite (Phoslock®, a widely used PISM for endogenous P release control) at pH 5, 7, 8, and 9 were calculated to be 0.88, 0.59, 0.41, and 0.39 mg/g min using Eq. (3). Clearly, the initial $H_zPO_4^{z-3}$ adsorption rate of LH was larger than that of Phoslock®. Thus, from the point of view of the $H_zPO_4^{z-3}$ uptake rate, LH has a higher potential to be applied as a PISM for $H_zPO_4^{z-3}$ elimination from water than Phoslock®.

The isotherm of $H_zPO_4^{z-3}$ adsorption by LH is displayed in Fig. 2b. The computed values of isotherm model parameters for $H_zPO_4^{z-3}$ adsorption onto LH are presented in Table 2. According to Fig. 2b and Table 2, the Freundlich

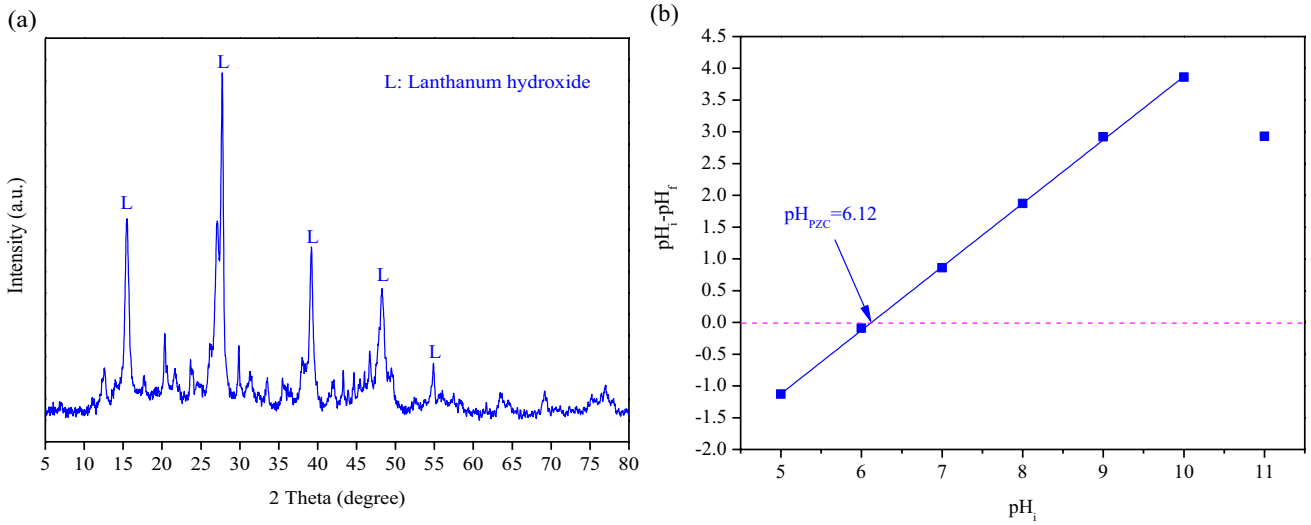

Fig. 1 (**a**) XRD pattern and (**b**) pH_{PZC} of LH

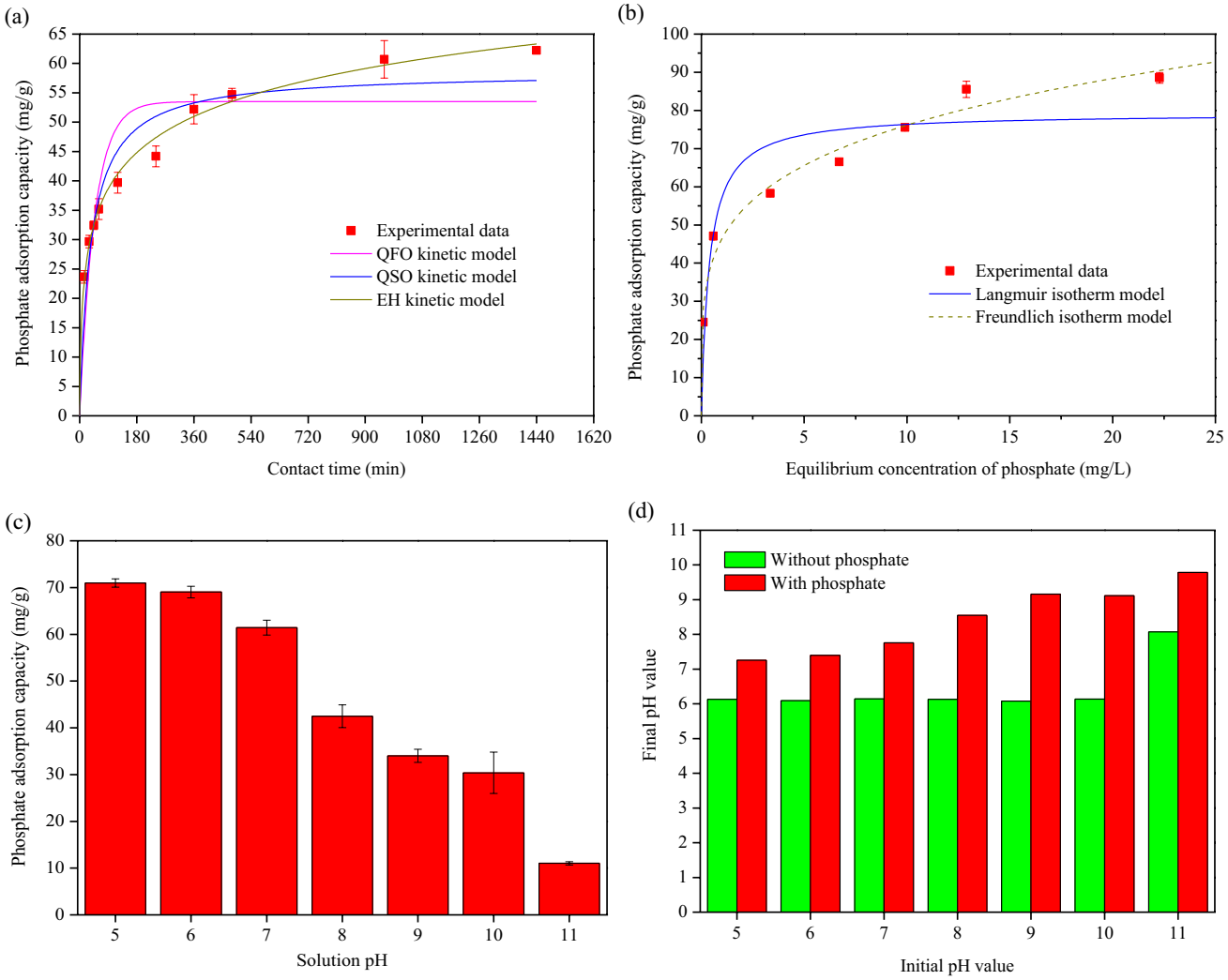

Fig. 2 Adsorption (**a**) kinetics and (**b**) isotherm of $H_zPO_4^{z-3}$ onto LH, (**c**) effect of pH on $H_zPO_4^{z-3}$ adsorption onto LH, and (**d**) final pH values of solutions after their contact with LH in the absence and presence of $H_zPO_4^{z-3}$.

isotherm model ($R^2 = 0.964$) can better describe the adsorption isotherm of $H_zPO_4^{z-3}$ on LH than the Langmuir isotherm model ($R^2 = 0.809$). The value of $1/n$ was less than 1, which demonstrates the beneficial adsorption of $H_zPO_4^{z-3}$ onto LH (Lu et al. 2022). The theoretically calculated greatest $H_zPO_4^{z-3}$ monolayer adsorption capacity for LH was 79.3 mg/g, which was larger than those of many other PISMs for phosphorus immobilization in sediment reported in previous researches (Fan et al. 2017; Haghseresht et al. 2009; Lei et al. 2021; Li et al. 2019; Lin et al. 2020a; Wang et al. 2015; Wu et al. 2022b; Xia et al. 2022; Yang et al. 2015; Yin et al. 2018b, 2020; Zhou et al. 2019) (Table 3). This suggests that from the point of view of the greatest $H_zPO_4^{z-3}$ uptake capacity, LH is a promising PISM for the suppression of endogenous phosphorus release into OW.

The impact of pH on $H_zPO_4^{z-3}$ adsorption by LH is shown in Fig. 2c. When the pH of solution rose from 5 to 9, the amount of $H_zPO_4^{z-3}$ adsorbed on LH decreased (Fig. 2c). As shown in Fig. 1b, the pH_{PZC} of LH was 6.12. At pH below 6.12, the surface of LH possesses net positive charges. As the pH of solution rose from 5 to 6, the electrostatic attraction force between $H_zPO_4^{z-3}$ and LH decreased, resulting in the decreased $H_zPO_4^{z-3}$ adsorption capacity. At pH above 6.12, the surface of LH possessed net negative charges. When the solution pH rose from 6 to 7, the electrostatic attraction force changed to the electrostatic repulsion force, resulting in a decline in the $H_zPO_4^{z-3}$ adsorption performance. As the solution pH rose from 7 to 11, the electrostatic repulsion between $H_zPO_4^{z-3}$ and LH increased, which led to the decrease in the $H_zPO_4^{z-3}$ adsorption ability. Furthermore, the increased OH^- ions competed with $H_zPO_4^{z-3}$ for the active adsorption site on the surface of LH, which brought about the decreased $H_zPO_4^{z-3}$ adsorption capacity with the increasing solution pH (Zhang et al. 2022).

Table 1 Parameters of kinetics equations for $H_zPO_4^{z-3}$ adsorption by LH

Kinetic models	Parameter	Value
QFO kinetic model	$Q_{e,exp}$ (mg/g)	62.2
	$Q_{e,cal}$ (mg/g)	53.5
	k_1 (1/min)	0.0213
	R^2	0.713
QSO kinetic model	$Q_{e,exp}$ (mg/g)	62.2
	$Q_{e,cal}$ (mg/g)	58.5
	k_2 (g/mg min)	0.000483
	h (mg/g min)	1.65
	R^2	0.882
EH kinetic model	a (mg/g min)	7.45
	b (g/mg)	0.112
	R^2	0.988

$Q_{e,exp}$ represents the experimental value of Q_e, and $Q_{e,cal}$ represents the calculated value of Q_e

Table 2 Parameters of isotherm equations for $H_zPO_4^{z-3}$ adsorption onto LH

Isotherm model	Parameter	Value
Langmuir isotherm model	Q_m (mg/g)	79.3
	K_L (L/mg)	2.59
	R^2	0.809
Freundlich isotherm model	K_F	46.4
	$1/n$	0.215
	R^2	0.964

Compared to HPO_4^{2-}, $H_2PO_4^-$ tends to be easily adsorbed onto metal oxide owing to its low adsorption free energy (Zhang et al. 2022). When pH increased from 5 to 11, the concentration of $H_2PO_4^-$ decreased, resulting in the decrease in the $H_zPO_4^{z-3}$ adsorption capacity. The final solution pH value after the addition of LH in the presence of $H_zPO_4^{z-3}$ was higher than that in the absence of $H_zPO_4^{z-3}$ (Fig. 2d). This indicates that OH^- is released from LH as a result of ligand exchange. Thus, ligand exchange is an important mechanism for $H_zPO_4^{z-3}$ adsorption onto LH over the pH range of 5–11.

In order to deeply understand the mechanism for the interaction between $H_zPO_4^{z-3}$ and LH, the XPS analyses on the original and $H_zPO_4^{z-3}$-adsorbed LH samples were implemented and the results are given in Fig. 3. The peaks of C 1 s, O 1 s, and La 3 d were observed in the full XPS spectra of LH samples prior to and after reaction with $H_zPO_4^{z-3}$, and the peak of P 2p was only observed in the full XPS spectrum of LH sample after reaction with $H_zPO_4^{z-3}$ (Fig. 3a). This suggests that $H_zPO_4^{z-3}$ has been adsorbed by LH successfully after the contact of $H_zPO_4^{z-3}$ solution with LH. As Fig. 3b shows, the P 2p peak for the $H_zPO_4^{z-3}$-adsorbed LH was located at 133.31 eV. The binding energy of P 2p XPS peak for the LH sample after the adsorption of $H_zPO_4^{z-3}$ was larger than those for the $H_zPO_4^{z-3}$ bound to the $-N^+(CH_3)_3$ groups of cationic hydrogel by electrostatic attraction (131.9 eV) (Dong et al. 2017) and $NaH_2PO_4{\cdot}2H_2O$ reference salt (132.6 eV) (Liu et al. 2020; Mallet et al. 2013). This demonstrates that compared to the electrostatic attraction force, the interaction force between $H_zPO_4^{z-3}$ and LH is stronger, and the primary mechanisms that dominate the adsorption of $H_zPO_4^{z-3}$ by LH include the formation of inner-sphere phosphate-lanthanum complex. The La 3d5/2 spectra (Fig. 3c) revealed peaks shift from 834.74 and 838.58 eV to 834.98 and 838.52 eV, respectively. The La 3d3/2 spectra (Fig. 3c) revealed peaks shift from 851.54 and 855.50 eV to 851.84 and 855.38 eV, respectively. These results further confirm the formation of inner-sphere

Table 3 Maximum $H_zPO_4^{z-3}$ adsorption capacities for LH in this study and other PISMs in previous researches

Number	Name	Maximum adsorption capacity (mg/g)	Reference
1	Phoslock®	9.47–10.54	Haghseresht et al. 2009
2	Lanthanum-modified zeolite	64.1	Li et al. 2019
3	Aluminum/lanthanum co-modified attapulgite	10.6	Yin et al. 2020
4	Zirconium-modified zeolite	10.2	Yang et al. 2015
5	Zirconia/zeolite composite	22.62	Fan et al. 2017
6	Ca/Fe-layered double hydroxide-zeolite composite	46.7	Wu et al. 2022b
7	Amended calcium peroxide material	29.28	Zhou et al. 2019
8	Iron rich glauconite sand	0.65–1.23	Xia et al. 2022
9	Aluminum/iron co-modified calcite	27	Lei et al. 2021
10	Drinking water treatment sludge	7.46	Wang et al. 2015
11	Aluminum-modified attapulgite	8.79	Yin et al. 2018b
12	Zirconia/magnetite/zeolite composite	4.1	Lin et al. 2020a

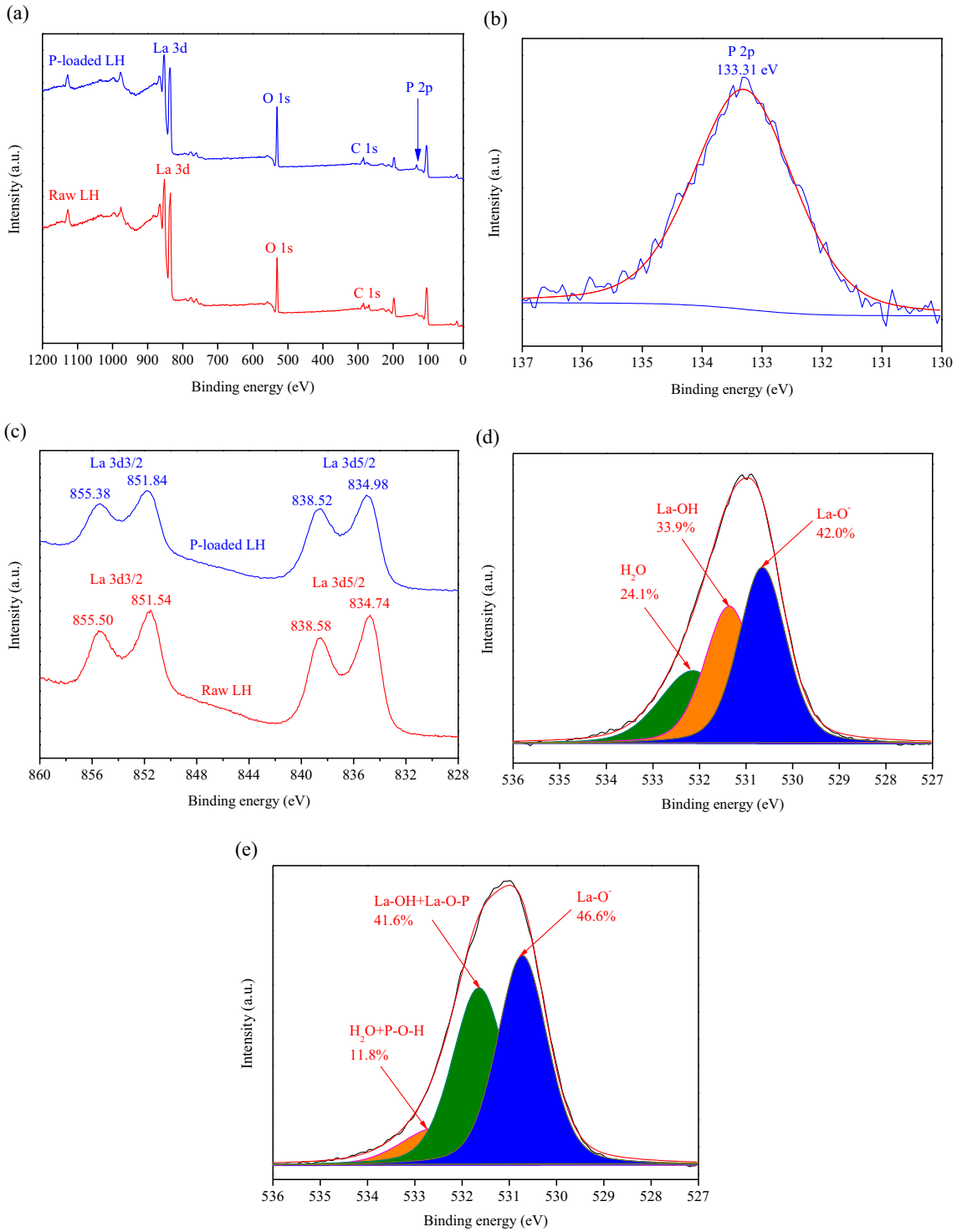

Fig. 3 XPS spectra of raw and $H_zPO_4^{z-3}$-adsorbed LH samples: (**a**) full-scan XPS spectra of LH samples prior to and after $H_zPO_4^{z-3}$ adsorption; (**b**) P 2p XPS spectrum of $H_zPO_4^{z-3}$-adsorbed LH; La 3d XPS spectra of LH samples prior to and after $H_zPO_4^{z-3}$ adsorption; O 1 s XPS spectra of (**d**) raw and (**e**) $H_zPO_4^{z-3}$-adsorbed LH samples

La–O-P complexes after the uptake of $H_zPO_4^{z-3}$ by LH. As Fig. 3d shows, the O 1 s peak of the raw LH was fitted as three overlapping peaks attributed to oxygen bonded lanthanum (La–O^-), lanthanum-bonded hydroxyl group (La-OH), and adsorbed water molecules (H_2O), respectively (Liu et al. 2022). As Fig. 3e shows, the O 1 s peak of the

$H_zPO_4^{z-3}$-adsorbed LH was fitted as three overlapping peaks ascribed to La–O^-, La-OH + La–O-P, and H_2O + P-O–H, respectively (Cheng et al. 2022; Min et al. 2019; Qu et al. 2023; Yuan et al. 2018). The relative area of La-OH for the raw LH was lower than that of La-OH + La–O-P for the $H_zPO_4^{z-3}$-adsorbed LH (Fig. 3d and e). This indicates the formation of inner-sphere La–O-P complex after the uptake of $H_zPO_4^{z-3}$ by LH.

All the results mentioned above reveal that the ligand exchange and inner-sphere lanthanum-phosphate complex formation act as a vital role in the uptake of $H_zPO_4^{z-3}$ from aqueous solution by LH at pH 7.

Effect of capping mode on control of P release from sediment by LH without SPM deposition

DO, pH, DRP, and DTP of OW

The changes of DO, pH, DRP, and DTP in OW for the control, one-time LH capping, and multiple LH capping groups without SPM deposition with incubation time are given in Fig. 4. The reduction rates of DRP and DTP from OW by the LH capping in the absence of SPM deposition are also given in Fig. 4. As Fig. 4a shows, in the absence of SPM deposition, the concentrations of DO in OW for the control, one-time LH capping, and multiple LH capping groups were less than 0.6 mg/L, except for that of OW in the multiple capping group on the 5th day, meaning that the sediments for the control, one-time capping, and multiple capping groups without SPM deposition were incubated in anoxic state during the period of 10–197 days' incubation. As Fig. 4b shows, the pH values of OW for the control, one-time LH capping, and multiple LH capping groups without SPM deposition were in the ranges of 6.51–7.36, 6.06–7.38, and 6.50–8.44, respectively. In the absence of SPM deposition, although the one-time or multiple LH capping had a certain impact on the OW pH in the early stage of application, it had an insignificant influence on the OW pH during the later period of application (Fig. 4b). As Fig. 4c and e show, the concentrations of DRP and DTP in OW for the control group under no SPM deposition condition fluctuated between 0.055 and 0.705 mg/L during 5–197 days' incubation period and between 0.092 and 0.710 mg/L during 10–186 days' incubation period, respectively, which were higher than the initial DRP and DTP concentrations. Furthermore, when the experimental time rose from 10 to 30 days, from 45 to 50 days and from 120 to 186 days, the DRP and DTP concentrations increased. These results demonstrate that the liberation of internal P can take place under anoxic conditions. From Fig. 4c and e, it also can be seen that the concentration of DTP in OW for the control group without SPM deposition was close to that of DRP, suggesting that the P in OW that is released from sediment exists in the form of inorganic P. As shown in Fig. 4c and e, in the absence of SPM deposition, the concentrations of DRP and DTP in OW significantly decreased after the one-time or multiple LH capping. The elimination rates of DRP from OW by the one-time and multiple LH capping without SPM deposition were found to be 77.3–100% and 47.9–100%, respectively (Fig. 4d), and those of DTP by the one-time and multiple LH capping were 84.9–100% and 78.7–100%, respectively (Fig. 4f). These results indicate that the one-time and multiple LH capping both can effectively block the release of internal phosphorus from sediment into OW under anoxia conditions in the absence of SPM deposition. From Fig. 4c–f, it was also observed that under no SPM deposition condition, the restraint efficiency of endogenous phosphorus release into OW by the one-time LH capping was higher than that by the multiple LH capping during the early period of application, but the restraint efficiency of internal phosphorus release into OW by the former was equal to or lower than that by the latter during the later period of application on the whole. This means that under no SPM deposition condition, although the transformation of covering mode from one-time covering to multiple covering has an insignificant negative effect on the performance of LH to resist the endogenous phosphorus release to OW during the later period of application, it decreases the interception efficiency of LH in the early stage of application.

DGT-labile P and Fe in OW/sediment profile

It is universally known that although the mechanisms of internal phosphorus release are numerous and complex, two basic sub-processes are included in the migration process of internal phosphorus from sediment to OW (Ding et al. 2015; Wang et al. 2023; Yu et al. 2017). One basic sub-process is the supply of phosphorus from sediment to pore water (PW) (Ding et al. 2015; Yu et al. 2017). The other basic sub-process is the transport of the soluble phosphorus from PW into OW via a molecular diffusion mechanism (Ding et al. 2015; Yu et al. 2017). The flux of P liberation from sediment to OW can be assessed by using the Fick diffusive law (Ding et al. 2023). A DRP gradient in PW is critical to the determination of the phosphorus diffusion flux from sediment to OW across the interface between sediment and OW (Chen et al. 2021a; Ding et al. 2023). In general, the reductive dissolution of Fe(III) (oxy)hydroxides is a predominant mechanism that governs the liberation of iron-bound phosphorus into PW under anoxia condition (Chen et al. 2019; Wu et al. 2021; Yuan et al. 2020).

In order to further evaluate the performance of LH capping to intercept endogenous phosphorus liberation into OW in the absence of SPM deposition and determine the interception mechanism, the impact of one-time and multiple LH capping on the concentrations of UP_{DGT} and UF_{DGT} in the

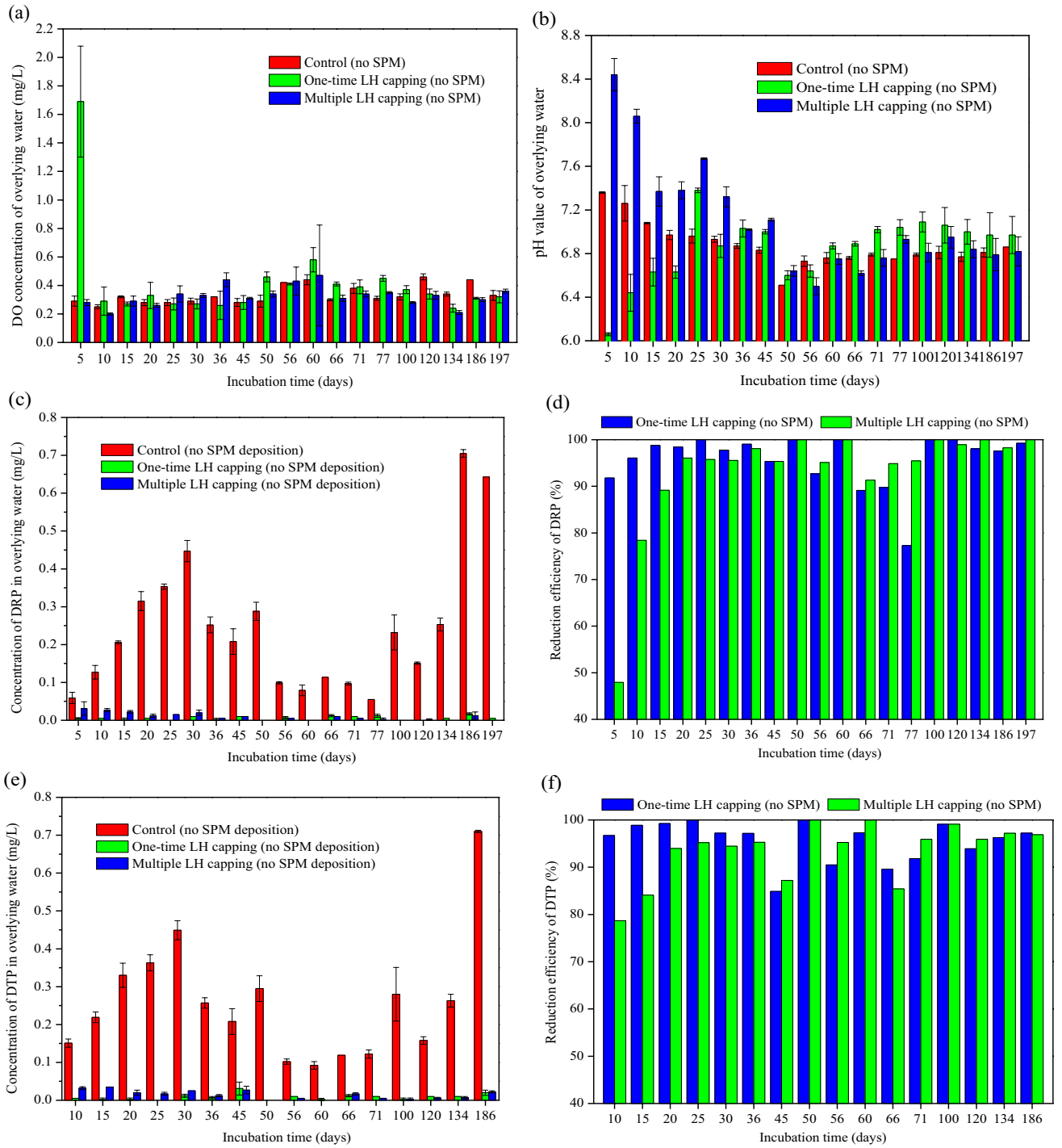

Fig. 4 Changes in (**a**) DO, (**b**) pH, (**c**) DRP, and (**e**) DTP of OW in control, one-time capping, and multiple capping groups in the absence of SPM deposition; reduction efficiencies of (**d**) DRP and (**f**) DTP by one-time and multiple capping in the absence of SPM deposition

profile of sediment and OW without SPM deposition was investigated. The obtained results are displayed in Fig. 5. As Fig. 5a shows, the concentrations of UP_{DGT} in OW and sediment ranged from 0.189 to 0.326 mg/L and from 0.263 to 0.505 mg/L, respectively. The average concentrations of UP_{DGT} in OW and sediment were calculated to be 0.234 and 0.417 mg/L, respectively. These results demonstrate that in the absence of SPM deposition, the liberation of internal P from sediment to PW occurs under anoxia condition, and the P in the PW can be diffused into OW via the molecular diffusion mechanism. After the one-time or multiple LH capping, the UP_{DGT} concentration of OW was substantially

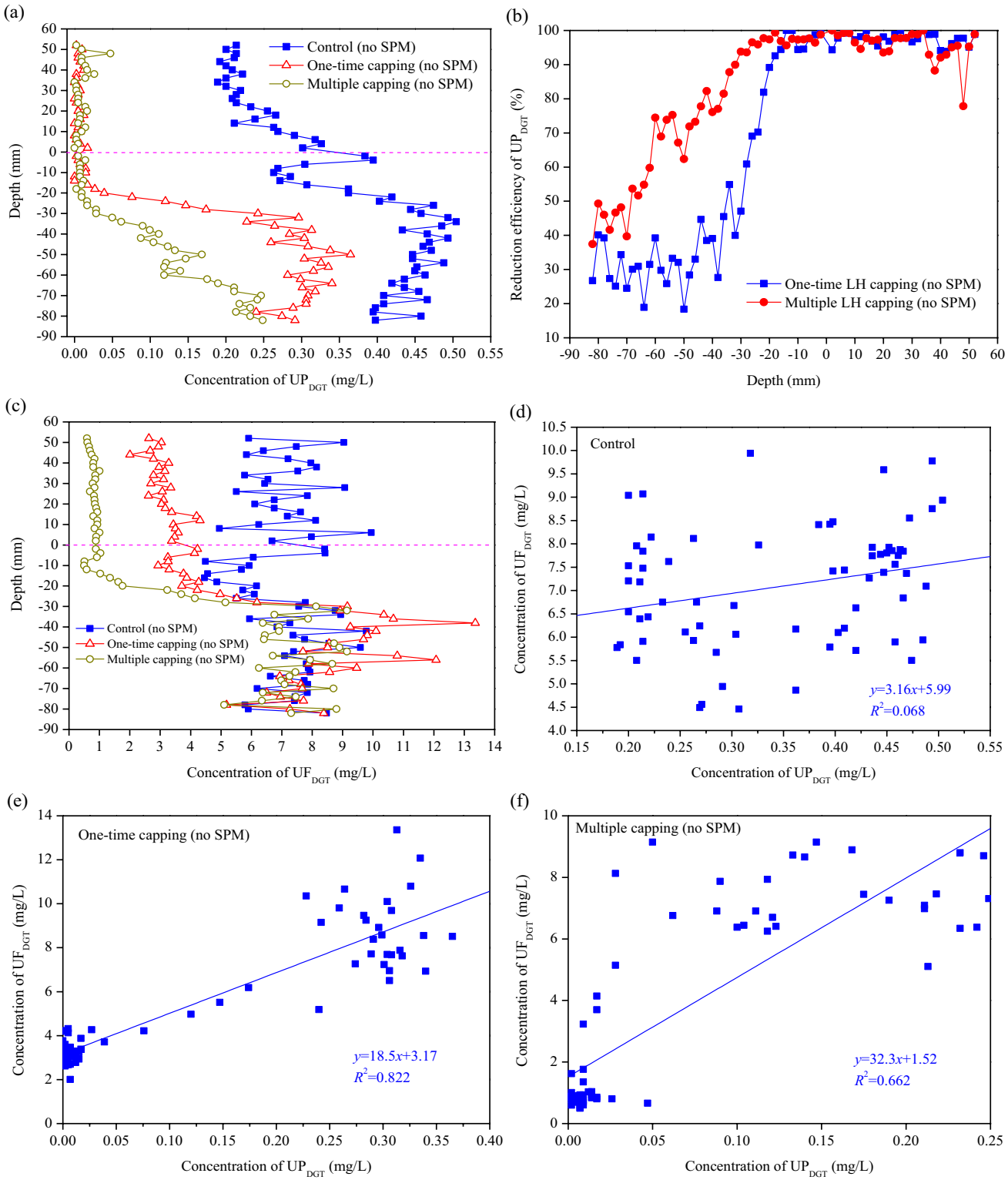

Fig. 5 Distributions of (**a**) UP_{DGT} and (c) UF_{DGT} in the profile of OW and sediment in the absence of SPM deposition; (**b**) reduction rates of UP_{DGT} by one-time and multiple capping in the absence of SPM deposition; relationship between UP_{DGT} and UF_{DGT} for (**d**) control, (**e**) one-time capping, and (**f**) multiple capping groups in the absence of SPM deposition

decreased (Fig. 5a). The elimination efficiencies of UP_{DGT} in OW by the one-time and multiple LH capping were found to be 93.9–100% and 77.8–100%, respectively (Fig. 5b), which further indicates that the one-time and multiple LH capping both can effectively hinder the transport of internal phosphorus from sediment into OW during the later period of application. The one-time and multiple LH capping also can effectively reduce the UP_{DGT} concentration of sediment (Fig. 5a and b). However, the reduction rate of UP_{DGT} in sediment by the one-time and multiple LH capping was related to the sediment depth (Fig. 5b). The elimination efficiency of UP_{DGT} in the upper 18 mm sediment by the one-time LH covering was very high (92.6–100%), but the reduction efficiency tended to decrease until a relatively low value was achieved when the depth of sediment varied from -20 to -82 mm (the minus sign indicates the depth below the interface between OW and sediment) (Fig. 5b). The elimination efficiency of UP_{DGT} in the upper 30 mm sediment by the multiple LH covering was very high (93.6–99.3%), but the reduction efficiency showed decreased trend as the depth of sediment varied from -32 to -82 mm (Fig. 5b). These results indicate that regardless of whether the capping mode is the one-time or multiple capping, LH can inactivate the UP_{DGT} in the upper sediment. As shown in Fig. 5c, the concentrations of UF_{DGT} in OW ranged from 4.95 to 9.94 mg/L, and those in sediment were in the range of 4.46–9.78 mg/L. This demonstrates that phosphorus can be released from sediment into pore water (PW) through the mechanism of reductive dissolution of Fe(III) (oxy)hydroxides. The concentrations of UF_{DGT} in sediment for the one-time capping group ranged from 2.93 to 13.4 mg/L, and those for the multiple LH capping group ranged from 0.497 to 9.14 mg/L (Fig. 5c). In addition, for the one-time or multiple LH capping group, there was a relatively good relationship between the concentrations of UF_{DGT} and UP_{DGT} (Fig. 5e and f). These results indicate that under the condition of one-time or multiple LH capping, phosphorus still can be released from sediment into PW via the mechanism of reductive dissolution of Fe(III) (oxy)hydroxides. After the one-time and multiple LH capping, the capping layer can adsorb the DRP in PW via the mechanism of inner-sphere lanthanum-phosphate complex formation, giving rise to the reduction of the DRP concentration in the PW. This induces the release of P from UP_{DGT} to make up the decreased DRP concentration of PW. Compared to the liberation rate of phosphorus from UP_{DGT}, the adsorption rate of DRP onto LH should be larger. This results in the very low concentration of UP_{DGT} in the upper sediment and the relatively low concentration of UP_{DGT} in the lower sediment after the one-time and multiple LH capping under no SPM deposition condition.

The static and active layers can be applied to characterize the stratification features of PW DRP and UP_{DGT} (Lin et al. 2017). The P static layer (SL) has low concentrations of PW DRP and UP_{DGT}, while the concentrations of PW DRP and UP_{DGT} in the P active layer (AL) were higher than those in the P SL (Lin et al. 2017). Some previous studies found that the formation of P SL with low concentrations of DRP and UP_{DGT} in the upper sediment played a key role in the interception of endogenous phosphorus release into OW by Phoslock® (Wang et al. 2017), zirconium-modified bentonite (Lin et al. 2019a), magnetite-modified activated carbon (Lin et al. 2019c), and lanthanum/iron co-modified attapulgite (Qu et al. 2023). Therefore, the formation of P SL in the upper sediment due to the inactivation of UP_{DGT} by the LH capping layer played a significant role in the restraint of endogenous P release into OW by the one-time and multiple LH capping in the absence of SPM deposition. It should be noted that the P SL has two main parameters (Lin et al. 2017; Wang et al. 2017). One is the average concentrations of DRP and UP_{DGT} in the P SL (Lin et al. 2017; Wang et al. 2017). The other is the thickness of the P SL (Lin et al. 2017; Wang et al. 2017). Under the condition of one-time LH capping, the thickness of the P SL was 18 mm, and the mean UP_{DGT} concentration in the P SL was 0.010 mg/L. Under the condition of multiple LH capping, the thickness of the P SL was 30 mm, and the mean UP_{DGT} concentration in the P SL was 0.012 mg/L. It is obvious that the thickness of the P SL under the condition of multiple LH capping was larger than that under the condition of one-time LH capping, which means that the transformation of covering mode from the single high dose covering to the multiple smaller doses covering increases the ability for the immobilization of UP_{DGT} in the upper sediment in the later stage of application. This suggests that the change of capping mode from the one-time capping to the multiple capping conduces to the application of LH as a covering material to restrain the liberation of internal phosphorus into OW in the absence of SPM deposition in the long run.

The potential of P upward release from AL to SL (R_{AL}) was calculated using Eq. (9) (Lin et al. 2017):

$$R_{AL} = \frac{(\overline{C}_{AL} - \overline{C}_{SL}) \times \delta_{AL}}{\overline{C}_{SL} \times \delta_{SL}} \quad (9)$$

where $\overline{C}_{AL}$ and $\overline{C}_{SL}$ represent the average concentrations of PW DRP or UP_{DGT} in the P AL and SL, respectively (mg/L); δ_{AL} and δ_{SL} represent the thickness of the P AL and SL, respectively (mm). In the absence of SPM deposition, the R_{AL} values under the conditions of one-time and multiple LH capping were calculated to be 23.6 and 1.96, respectively. The R_{AL} value under the condition of multiple LH capping was much lower than that under the condition of one-time LH capping, which demonstrates that the stabilization of P in the static layer in the later stage of application increases when the capping mode changes from the one-time LH capping to the multiple LH capping. This also conduces

to the application of LH as an active covering material to restrain the endogenous phosphorus liberation into OW in the absence of SPM deposition in the long run.

P fractionation of sediment

The potential of endogenous P release has a close association with its fractionation (Yan et al. 2022). LI-P represents the immediately available P in sediment, and it is the loosely bound or exchangeable fraction of P (Ren et al. 2022; Ribeiro et al. 2008). RR-P indicates the P related to iron and manganese, and this form is mobile because it can be released under anoxic conditions (Cavalcante et al. 2018). OH-SRP indicates the P associated with metal (mainly aluminum and iron) oxides that can be exchangeable with hydroxyl ion, and it is relatively stable under common pH (5–9) and anoxia condition (Rydin 2000; Wang et al. 2013). H-P indicates the P related to apatite, calcium, and carbonates; and this form can be released only when the environment pH is acidic (Cavalcante et al. 2018). The probability of R-P release is low (Meis et al. 2012). To better understand how the one-time and multiple LH capping controls the endogenous P liberation into OW, the effect of the one-time and multiple LH capping under no SPM deposition condition on the speciation of P in sediment was researched, and the obtained result is listed in Fig. 6. In the absence of SPM deposition, the amounts of LI-P in the sediments for the control, one-time LH capping, and multiple LH capping groups were limited (Fig. 6a). Under no SPM deposition condition, the one-time LH capping decreased the amounts of RR-P, OH-SRP, and R-P in the 0–1 cm sediment layer, but increased the quantity of H-P in the 0–1 cm sediment layer (Fig. 6b–e). After the one-time LH capping in the absence of SPM deposition, the ratios of RR-P, OH-SRP, and R-P to P_{Total} in the 0–1 cm sediment layer decreased, but that of H-P to P_{Total} increased (Fig. 6f and g). These results mean that under no SPM deposition condition, the one-time LH capping can decrease the content of P_{Mobile} in the topmost sediment layer via the transformation of RR-P to H-P. After the multiple LH capping without SPM deposition, the amounts of RR-P and OH-SRP in the 0–1 cm sediment layer decreased, but the quantities of H-P and R-P in the 0–1 cm sediment layer increased (Fig. 6b–e). The multiple LH capping in the absence of SPM deposition brought about the decreased proportions of RR-P and OH-SRP to P_{Total} in the 0–1 cm sediment layer but the increased proportions of H-P and R-P to P_{Total} in the 0–1 cm sediment layer (Fig. 6f and h). Therefore, in the absence of SPM deposition, the multiple LH capping can reduce the quantity of P_{Mobile} in the topmost sediment layer by the way of the transformation of RR-P to H-P and R-P. The P_{Mobile} in sediment is regarded as the internal phosphorus loading of water bodies (Rydin 2000; Yin et al. 2022). Thus, the immobilization of P_{Mobile} in the topmost sediment layer played a significant role in the restraint of endogenous phosphorus liberation into OW by the one-time and multiple LH capping in the absence of SPM deposition.

Effect of capping mode on control of P release from sediment by LH with SPM deposition

DO, pH, DRP, and DTP of OW

The changes of DO, pH, DRP, and DTP in OW for the control, one-time LH capping, and multiple LH capping groups with SPM deposition with the incubation time are displayed in Fig. 7. The reduction rates of DRP and DTP in OW by the one-time and multiple LH capping with SPM deposition are also shown in Fig. 7. As depicted in Fig. 7a, the DO concentrations of OW in the control and multiple LH capping groups with SPM deposition during the whole sediment incubation period were lower than 0.5 mg/L. For the one-time LH capping group with SPM deposition, the DO concentration of OW was 1.79 mg/L on day 5, but after that, it was below 0.5 mg/L (Fig. 7a). These results indicate that the sediments for the control, one-time LH capping, and multiple LH capping groups with SPM deposition were maintained in anoxic conditions during the period of 10–197 days' incubation. As Fig. 7b shows, the pH values of OW for the control, one-time LH capping, and multiple LH capping groups with SPM deposition ranged from 6.58–7.59, 6.44–7.34, and 6.86–8.00, respectively, during the period of 5–197 days' incubation. As shown in Fig. 7c, under the condition of SPM deposition, with the increase in the incubation time from 5 to 20 days, from 25 to 30 days, from 60 to 66 days, and from 77 to 197 days, the DRP concentration of OW in the control group increased. This suggests that the liberation of internal P from sediment into OW under anoxia and SPM deposition condition occurs. As Fig. 7e shows, the concentrations of DTP in OW for the control group with SPM deposition were between 0.041 and 0.300 mg/L, which were higher than the initial DTP concentration of OW. In addition, when the incubation time rose from 60 to 66 days and from 100 to 186 days, the DTP concentration of OW for the control group with SPM deposition obviously increased (Fig. 7e). These results further suggest that during the sediment incubation period, the release of internal phosphorus into OW in anoxia environments under SPM deposition condition takes place. During the period of 5–50, 66–71, and 120–197 days' incubation, the one-time LH capping brought about the decrease in the concentration of DRP in OW under SPM deposition condition (Fig. 7c), and the elimination efficiencies were 5.88–84.1%, 7.14–35.7%, and 18.8–79.7%, respectively (Fig. 7d). During the period of 5–50, 60, 71, and 120–186 days' incubation, under SPM deposition conditions, the one-time LH capping

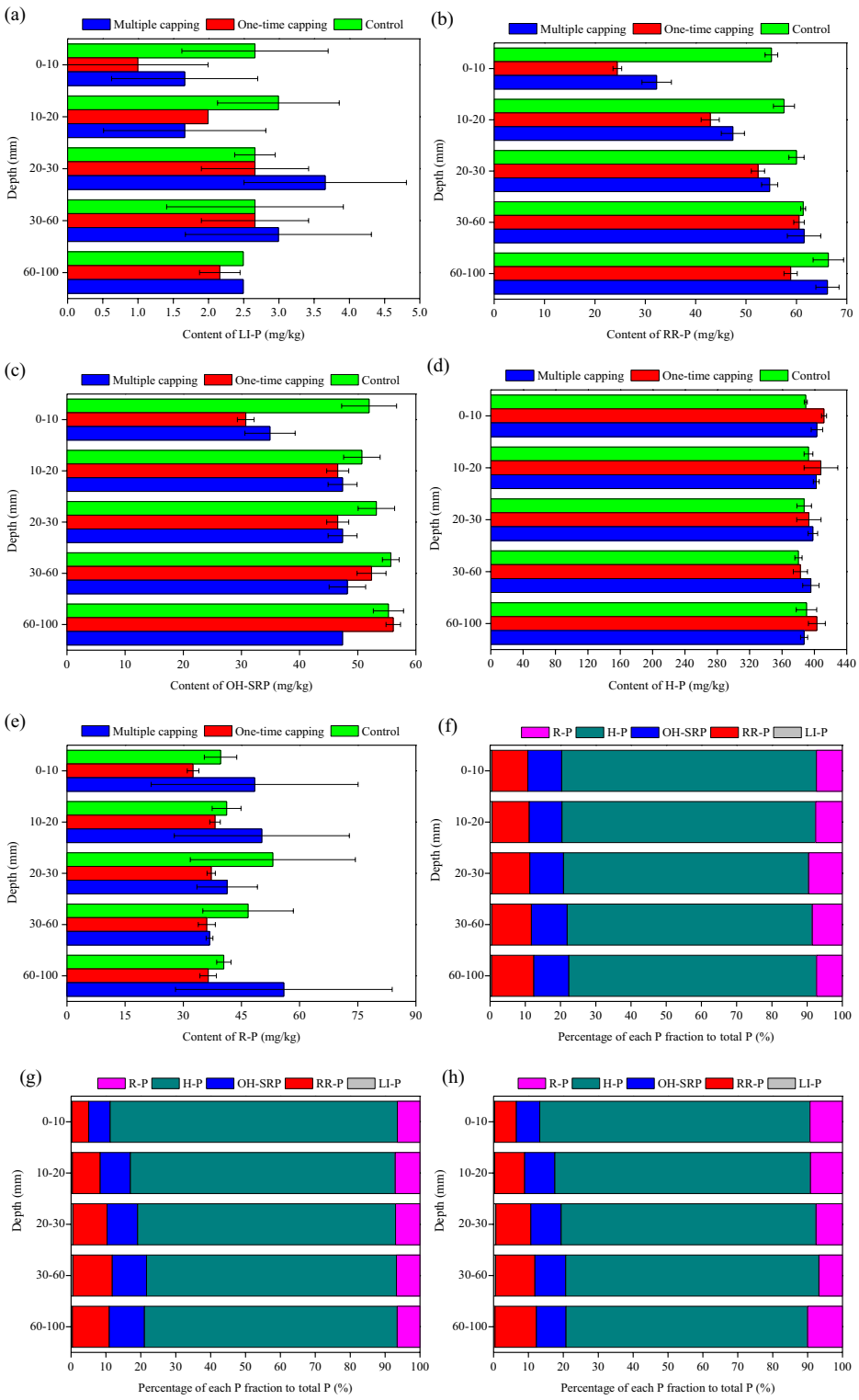

Fig. 6 Contents of (**a**) LI-P, (**b**) RR-P, (**c**) OH-SRP, (**d**) H-P, and (**e**) R-P in sediments from control, one-time capping, and multiple capping groups in the absence of SPM deposition; percentages of each P fraction to total P in sediments from (**f**) control, (**g**) one-time capping, and (**h**) multiple capping groups in the absence of SPM deposition

reduced the concentration of DTP in OW (Fig. 7e), and the elimination rates were 29.4–81.3%, 11.8%, 12.0%, and 21.8–67.2%, respectively (Fig. 7f). These results mean that in the presence of SPM deposition, the one-time LH capping has the capability to inhibit the release of endogenous phosphorus into OW during the early and later periods of application. Similarly, under SPM deposition conditions, the multiple LH capping can restrain the liberation of endogenous P into OW (Fig. 7c–f). However, under SPM deposition condition, the efficiency of endogenous phosphorus release

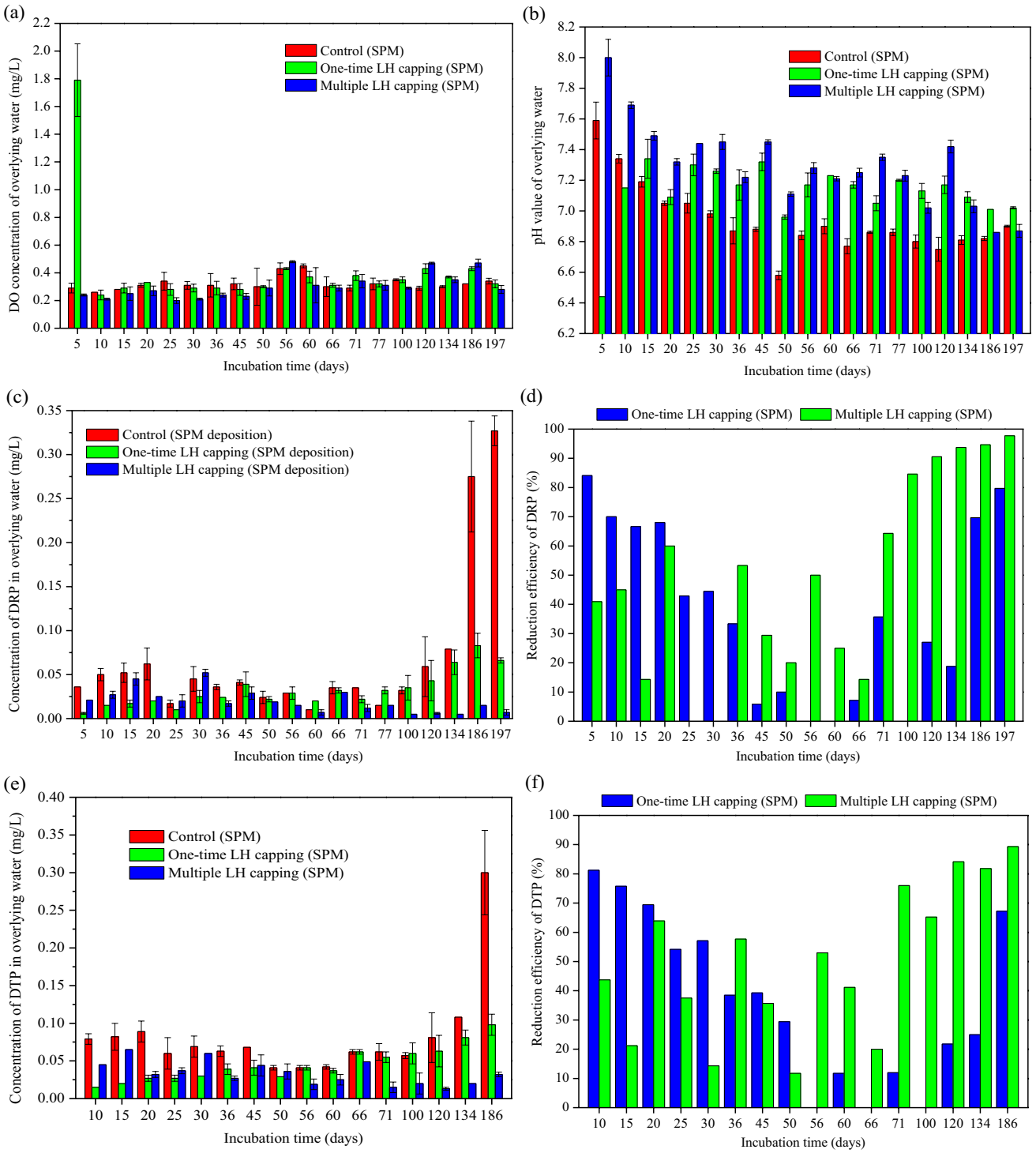

Fig. 7 Changes in (**a**) DO, (**b**) pH, (**c**) DRP, and (**e**) DTP of OW in control, one-time capping, and multiple capping groups under SPM deposition condition; reduction efficiencies of (**d**) DRP and (**f**) DTP by one-time and multiple capping under SPM deposition condition

into OW by the one-time LH capping was different to that by the multiple LH capping. From Fig. 7d and f, it was observed that under SPM deposition condition, the elimination rates of DRP and DTP in OW by the one-time LH capping in the early stage of application were higher than that by the multiple LH capping, but the elimination efficiencies of DRP and DTP in OW by the former in the later stage of application were lower than those by the latter. This demonstrates that under SPM deposition condition, although the change in the covering mode from the one-time high dose covering

to the multiple smaller doses covering reduces the controlling ability of endogenous phosphorus liberation into OW by LH during the early period of application, it enhances the performance of LH to reduce the endogenous phosphorus release to OW during the later period of application.

DGT-labile P and Fe in OW/sediment profile

To further evaluate the effectiveness of one-time and multiple LH covering to restraint the liberation of internal phosphorus into OW in the presence of SPM deposition and illustrate the interception mechanism, the impact of one-time and multiple LH capping on the concentrations of UP_{DGT} and UF_{DGT} in the OW/sediment profile was studied. The obtained results are given in Fig. 8. As observed from Fig. 8a, the concentrations of LP_{DGT} in OW and sediment for the control group with SPM deposition were in the range of 0.010–0.152 mg/L and 0.091–0.454 mg/L, respectively, with mean concentrations of 0.067 and 0.310 mg/L, respectively. Moreover, there were certain concentrations of UF_{DGT} in OW and sediment for the control group with SPM deposition (Fig. 8c), and the concentration of UF_{DGT} correlates to some extent with that of UP_{DGT} (Fig. 8d). These results demonstrate that phosphorus can be released from sediment via the mechanism of the reductive dissolution of Fe(III) (oxy)hydroxides under anoxic and SPM deposition condition. Under SPM deposition condition, the concentration of UP_{DGT} in OW at depths of between 2 and 34 mm decreased by 2.2–69.7% after the one-time LH capping, and the UP_{DGT} concentration of OW decreased by 64.0–100% after the multiple LH capping (Fig. 8a and b), demonstrating that the one-time and multiple LH capping can inhibit the endogenous P release into OW in the later stage of application under SPM deposition condition. Under SPM deposition condition, the concentration of UP_{DGT} in sediment decreased by 13.2–100% after the one-time LH capping, and it decreased by 5.6–98.3% after the multiple LH capping (Fig. 8a and b). This suggests that no matter whether the capping mode is the one-time capping or the multiple capping, the LH capping can inactivate the UP_{DGT} in sediment. This can be explained as follows. After the one-time or multiple LH capping, under SPM deposition condition, there were certain concentrations of UF_{DGT} in the OW/sediment profile, and the concentration of UF_{DGT} correlated to some extent with that of UP_{DGT}. This indicates that under LH capping and SPM deposition condition, phosphorus still can be released from sediment into PW due to the reductive dissolution of Fe(III) (oxy)hydroxides. However, the LH capping layer can adsorb the DRP in PW, which brought about the decreased DRP concentration in the PW. After the DRP concentration of PW decreased, the UP_{DGT} in sediment was released to compensate the decrease of the DRP concentration due to the adsorption of DRP by the LH capping layer. The rate of DRP concentration decrease due to the adsorption should be larger than the rate of P release from UP_{DGT}, resulting in that the concentration of UP_{DGT} in sediment under one-time or multiple LH capping condition was lower compared to that under no LH capping condition. Under the condition of no external P input, the P in OW came from sediment. The decrease in the UP_{DGT} concentration of sediment induced the decline in the diffusion flux of phosphorus from the sediment to the overlying water, thereby causing the decreased concentration of DRP, DTP, and UP_{DGT} in the overlying water after the one-time or multiple LH capping. Consequently, the inactivation of UP_{DGT} in sediment by LH was extremely important for the inhibition of endogenous phosphorus release from sediment to OW by the one-time and multiple LH capping under SPM deposition condition. It should be noted that under SPM deposition condition, the one-time and multiple LH capping resulted in the stratification of UP_{DGT} in the sediment profile, forming the phosphorus SL in the upper sediment (between -2 and -28 mm) and phosphorus AL in the lower sediment (between -30 and -82 mm). Obviously, the formation of phosphorus SL in the upper sediment acted as a significant role in the restraint of endogenous phosphorus release into OW by the one-time and multiple LH capping under SPM deposition condition.

Under SPM deposition condition, the average concentrations of UP_{DGT} in OW for the one-time and multiple LH capping groups were computed to be 0.0418 and 0.00535 mg/L, respectively. Clearly, under SPM deposition condition, the mean UP_{DGT} concentration of OW after the one-time LH capping was higher compared to that after the multiple LH capping. This further confirms that under SPM deposition condition, the change in the covering mode from the one-time covering to the multiple covering increases the efficiency of endogenous phosphorus liberation into OW by LH in the later period of application. Under SPM deposition condition, the UP_{DGT} concentrations of sediments at depths of between -2 and -14 mm for the one-time LH capping group were higher than those for the multiple LH capping group (Fig. 8a), and the UP_{DGT} reduction efficiency of the one-time LH capping was lower than that of the multiple LH capping (Fig. 8b). This indicates that the change in the covering mode from the one-time covering to the multiple covering increases the immobilization ability of UP_{DGT} in the topmost sediment by the LH covering layer during the later period of application. This is conductive to the utilization of LH as a capping material to restrain the endogenous phosphorus release into OW under SPM deposition condition in the long run.

P fractionation of sediment

To further illustrate the mechanism that governs the control of internal phosphorus liberation into OW by the one-time

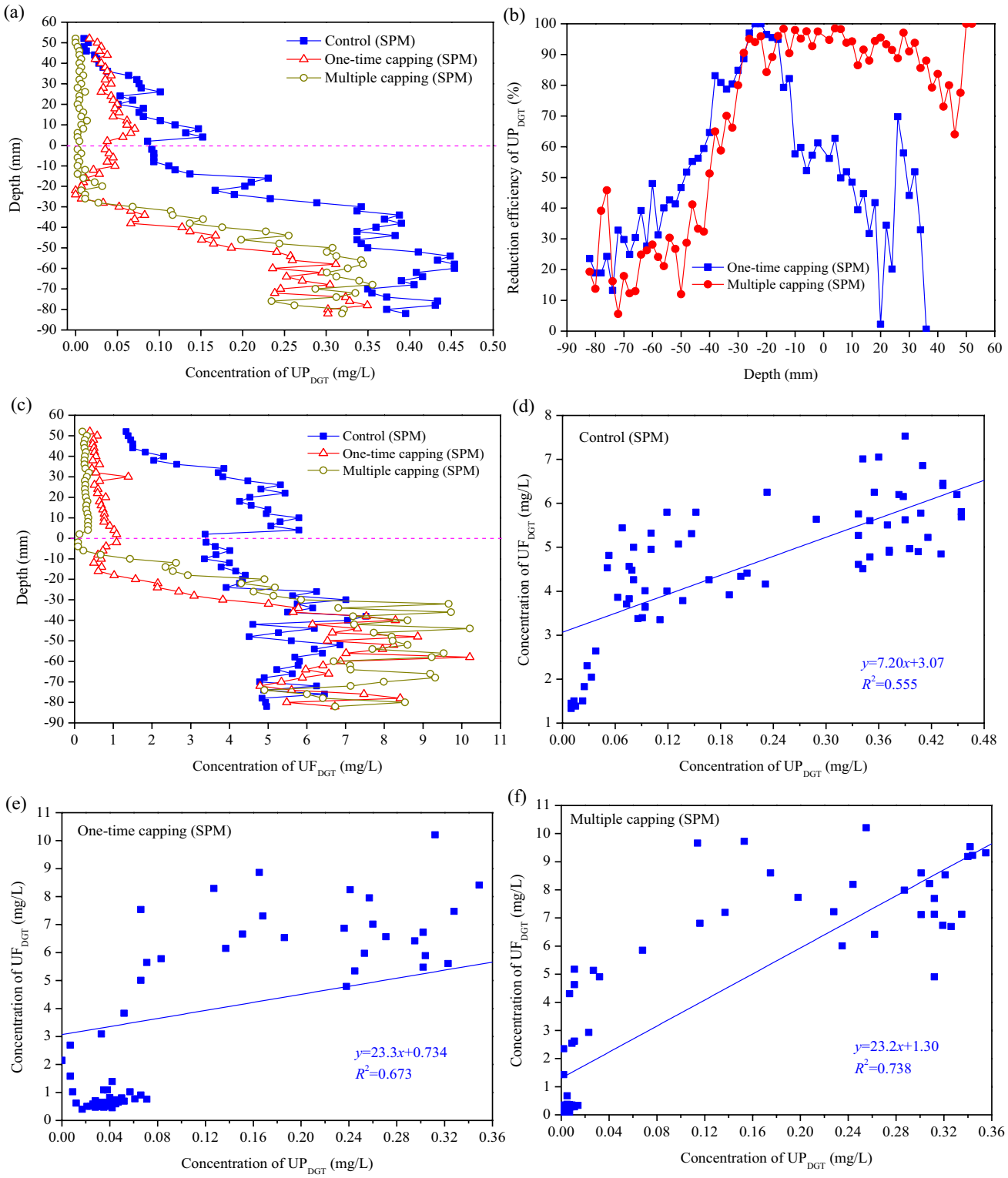

Fig. 8 Distributions of (**a**) UP_{DGT} and (**c**) UF_{DGT} in the profile of OW and sediment in the presence of SPM deposition; (**b**) reduction rates of UP_{DGT} by one-time and multiple capping under SPM deposition condition; relationship between UP_{DGT} and UP_{DGT} for (**d**) control, (**e**) one-time capping, and (**f**) multiple capping in the presence of SPM deposition

and multiple LH capping, the influence of one-time and multiple LH covering on the fractionation of phosphorus in sediment in the presence of SPM deposition was researched, and the results are displayed in Fig. 9. According to Fig. 9, we can make a conclusion that the one-time LH capping can reduce the P_{Mobile} in the topmost sediment by the transformation of RR-P to H-P, and the multiple LH capping can reduce the P_{Mobile} in the topmost sediment by the transformation of RR-P to H-P and R-P. Since the risk of phosphorus release from P_{Mobile} is high (Rydin 2000; Yin et al. 2022), the inactivation of P_{Mobile} in the topmost sediment by LH acted as a vital role in the restraint of endogenous phosphorus liberation to OW by the one-time and multiple LH capping under SPM deposition condition.

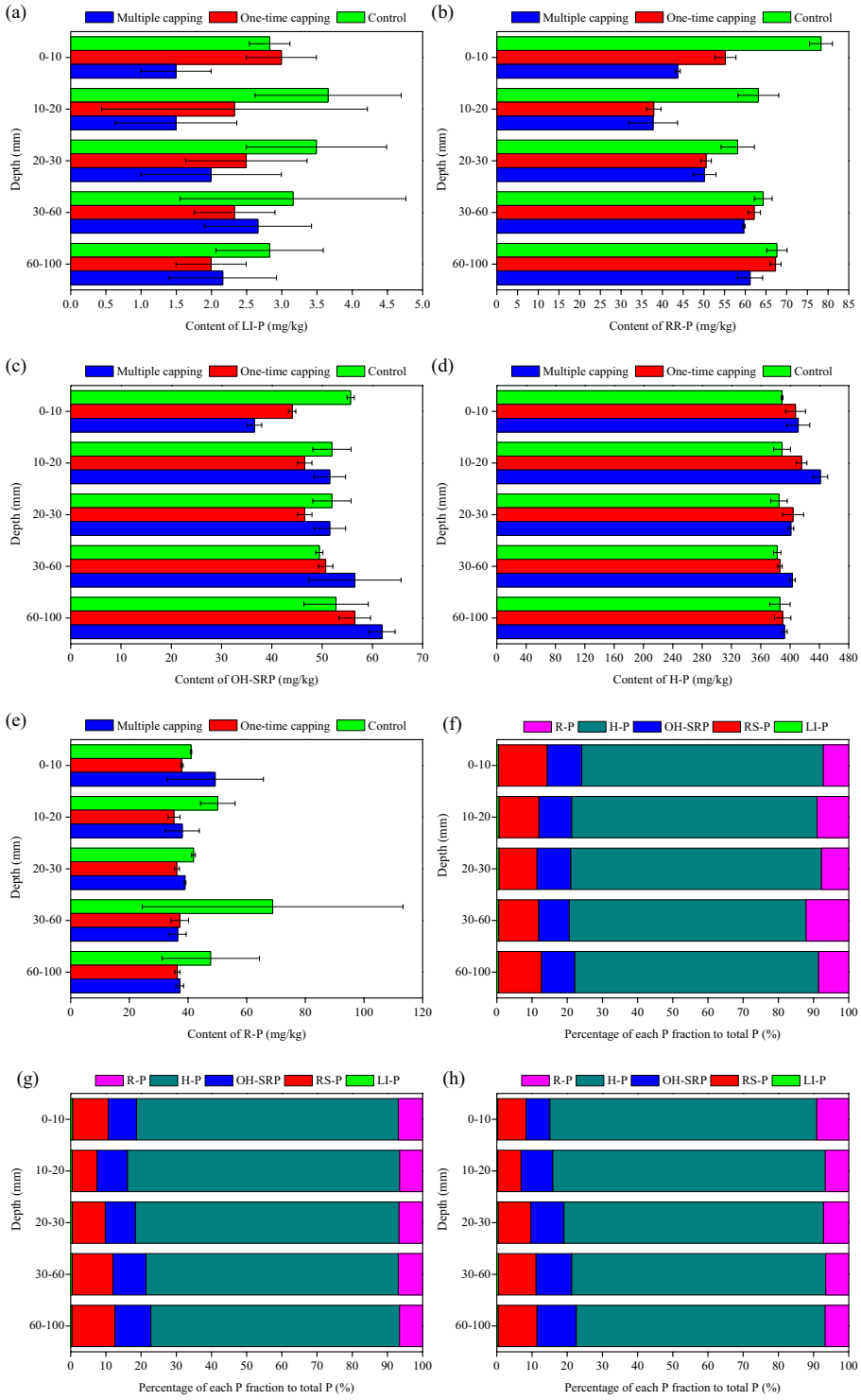

Fig. 9 Contents of (**a**) LI-P, (**b**) RR-P, (**c**) OH-SRP, (**d**) H-P, and (**e**) R-P in sediments from control, one-time capping, and multiple capping groups in the presence of SPM deposition; percentages of each P fraction to total P in sediments from (**f**) control, (**g**) one-time capping, and (**h**) multiple capping groups under SPM deposition condition

Implication for application of LH to control internal P release

This study observed that in the absence of SPM deposition, the one-time and multiple LH covering both can effectively restrain the migration of endogenous phosphorus into OW under anoxia condition. Therefore, LH has great potential to be used as a capping material to restrain endogenous phosphorus liberation into OW in the absence of SPM deposition. It should be noted that SPM is ubiquitous in aquatic environments (Ho et al. 2022; Walch et al. 2022). This work showed that in the presence of SPM deposition, the one-time or multiple LH capping still had the capability to mitigate the risk of endogenous phosphorus release into OW under anoxia condition. Furthermore, under SPM deposition condition, although the change of the covering mode from the one-time high dose covering to the multiple smaller doses covering led to the decline in the efficiency of LH to resist the release of internal phosphorus during the early period of application, it increased the performance of LH to suppress phosphorus release from sediment into OW during the later period of application. Therefore, the multiple LH capping has high potential to be used as a sediment remediation strategy for reducing the risk of internal phosphorus release from sediment in surface water bodies where SPM deposition often takes places in the long run.

Conclusions

(1) In the absence of SPM deposition, the one-time and multiple LH capping can effectively restrain the internal phosphorus release to OW under anoxia conditions, and the immobilization of UP_{DGT} and P_{Mobile} in the topmost sediment acted a significant role in the restraint of internal phosphorus release into OW by the LH capping
(2) In the absence of SPM deposition, although the change in the covering mode from the one-time high dose covering to the multiple smaller doses covering brought about a certain negative influence on the performance of LH to intercept the release of internal phosphorus from sediment into OW during the early period of application, it increased the ability of LH to inactivate UP_{DGT} in sediment during the later period of application
(3) Under SPM deposition condition, the one-time and multiple LH capping had the capability to mitigate the risk of phosphorus release from sediment into OW during anoxia, and the inactivation of UP_{DGT} and P_{Mobile} in the topmost sediment acted as a vital role in the mitigation in the risk of endogenous phosphorus liberation into OW by the LH capping
(4) Under SPM deposition condition, the change of the covering mode from the one-time covering to the multiple covering reduced the efficiency of endogenous P liberation into OW by LH under the circumstance of anoxia during the early period of application, it increased the controlling efficiency of LH capping during the later period of application
(5) The multiple LH capping is a promising approach for reducing the internal phosphorus release from sediments in surface water bodies where SPM deposition often occurs in the long run.

Supplementary Information The online version contains supplementary material available at https://doi.org/10.1007/s11356-023-28102-x.

Author contribution All authors contributed to the study conception and design. Material preparation, data collection, and analysis were performed by Fujun Sun, Jianwei Lin, and Yanhui Zhan. The first draft of the manuscript was written by Jianwei Lin, Fujun Sun, and Yanhui Zhan. All authors commented on previous versions of the manuscript. All authors read and approved the final manuscript.

Funding This work was financially supported by the National Science Foundation of China (Grant Nos. 51408354 and 50908142), the Capacity Building Project of Some Local Universities of Shanghai Science and Technology Commission (Grant Nos. 10230502900 and 20050501600), and the Program for Shanghai Collaborative Innovation Center for Cultivating Elite Breeds and Green-culture of Aquaculture animals (Grant No. 2021-kJ-02–12).

Data availability All data generated or analyzed during this study are included in this published article.

Declarations

Ethical approval Not applicable.

Consent to participate Not applicable.

Consent for publication Not applicable.

Conflict of Interest The authors declare no competing interests.

References

Abel S, Nybom I, Mäenpää K, Hale SE, Cornelissen G, Akkanen J (2017) Mixing and capping techniques for activated carbon based sediment remediation-efficiency and adverse effects for Lumbriculus variegatus. Water Res 114:104–112

Afridi MN, Lee W-H, Kim J-O (2019) Effect of phosphate concentration, anions, heavy metals, and organic matter on phosphate adsorption from wastewater using anodized iron oxide nanoflakes. Environ Res 171:428–436

Asaoka S, Kawakami K, Saito H, Ichinari T, Nohara H, Oikawa T (2021) Adsorption of phosphate onto lanthanum-doped coal fly ash—blast furnace cement composite. J Hazard Mater 406:124780

Balasuriya BTG, Ghose A, Gheewala SH, Prapaspongsa T (2022) Assessment of eutrophication potential from fertiliser application in agricultural systems in Thailand. Sci Total Environ 833:154993

Carpenter SR (2008) Phosphorus control is critical to mitigating eutrophication. Proc Natl Acad Sci USA 105:11039–11040

Cavalcante H, Araújo F, Noyma NP, Becker V (2018) Phosphorus fractionation in sediments of tropical semiarid reservoirs. Sci Total Environ 619–620:1022–1029

Chen M, Ding S, Liu L, Xu D, Gong M, Tang H, Zhang C (2016) Kinetics of phosphorus release from sediments and its relationship with iron speciation influenced by the mussel (Corbicula fluminea) bioturbation. Sci Total Environ 542:833–840

Chen Q, Chen J, Wang J, Guo J, Jin Z, Yu P, Ma Z (2019) In situ, high-resolution evidence of phosphorus release from sediments controlled by the reductive dissolution of iron-bound phosphorus in a deep reservoir, southwestern China. Sci Total Environ 666:39–45

Chen C, Wang Y, Pang X, Long L, Xu M, Xiao Y, Liu Y, Yang G, Deng S, He J, Tang H (2021a) Dynamics of sediment phosphorus affected by mobile aeration: pilot-scale simulation study in a hypereutrophic pond. J Environ Manage 297:113297

Chen X, Liu L, Yan W, Li M, Xing X, Li Q, Zhu L, Wu T, He X (2021b) Effects of nFe_3O_4 capping on phosphorus release from sediments in a eutrophic lake. Environ Sci Pollut Res 28:47056–47065

Cheng P, Liu Y, Yang L, Wang X, Chi Y, Yuan H, Wang S, Ren Y-X (2022) Adsorption and recovery of phosphate from aqueous solution by katoite: performance and mechanism. Colloid Surface A 655:130285

Determan RT, White JD, McKenna LW (2021) Quantile regression illuminates the successes and shortcomings of long-term eutrophication remediation efforts in an urban river system. Water Res 202:117434

Ding SM, Han C, Wang YP, Yao L, Wang Y, Xu D, Sun Q, Williams PN, Zhang CS (2015) In situ, high-resolution imaging of labile phosphorus in sediments of a large eutrophic lake. Water Res 74:100–109

Ding S, Sun Q, Chen X, Liu Q, Wang D, Lin J, Zhang C, Tsang DCW (2018) Synergistic adsorption of phosphorus by iron in lanthanum modified bentonite (Phoslock®): new insight into sediment phosphorus immobilization. Water Res 134:32–43

Ding Y, Yi Q, Jia Q, Zhang J, Zhou Z, Liu X (2023) Quantifying phosphorus levels in water columns equilibrated with sediment particles in shallow lakes: from algae/cyanobacteria-available phosphorus pools to pH response. Sci Total Environ 868:161694

Dong S, Wang Y, Zhao Y, Zhou X, Zheng H (2017) $La^{3+}/La(OH)_3$ loaded magnetic cationic hydrogel composites for phosphate removal: effect of lanthanum species and mechanistic study. Water Res 126:433–441

Fan Y, Li Y, Wu D, Li C, Kong H (2017) Application of zeolite/hydrous zirconia composite as a novel sediment capping material to immobilize phosphorus. Water Res 123:1–11

Fan X, Xing X, Ding S (2021) Enhancing the retention of phosphorus through bacterial oxidation of iron or sulfide in the eutrophic sediments of Lake Taihu. Sci Total Environ 791:148039

Fang L, Shi Q, Nguyen J, Wu B, Wang Z, Lo IMC (2017) Removal mechanisms of phosphate by lanthanum hydroxide nanorods: investigations using EXAFS, ATR-FTIR, DFT, and surface complexation modeling approaches. Environ Sci Technol 51:12377–12384

Fang L, Liu R, Li J, Xu C, Huang L-Z, Wang D (2018) Magnetite/lanthanum hydroxide for phosphate sequestration and recovery from lake and the attenuation effects of sediment particles. Water Res 130:243–254

Feng K, Deng W, Zhang Y, Tao K, Yuan J, Liu J, Li Z, Lek S, Wang Q, Hugueny B (2023) Eutrophication induces functional homogenization and traits filtering in Chinese lacustrine fish communities. Sci Total Environ 857:159651

Fuchs E, Funes A, Saar K, Reitzel K, Jensen HS (2018) Evaluation of dried amorphous ferric hydroxide CFH-12® as agent for binding bioavailable phosphorus in lake sediments. Sci Total Environ 628–629:990–996

Haghseresht F, Wang S, Do DD (2009) A novel lanthanum-modified bentonite, Phoslock, for phosphate removal from wastewaters. Appl Clay Sci 46:369–375

He Q, Zhao H, Teng Z, Wang Y, Li M, Hoffmann MR (2022) Phosphate removal and recovery by lanthanum-based adsorbents: a review for current advances. Chemosphere 303:134987

Ho QN, Fettweis M, Spencer KL, Lee BJ (2022) Flocculation with heterogeneous composition in water environments: a review. Water Res 213:118147

Hong S-H, Lee C-G, Park S-J (2022) Application of calcium-rich mineral under nonwoven fabric mats and sand armor as cap layer for interrupting N and P release from river sediments. Environ Sci Pollut Res 29:59444–59455

Hu M, Sardans J, Le Y, Yan R, Zhong Y, Peñuelas J (2022) Effects of wetland types on dynamics and couplings of labile phosphorus, iron and sulfur in coastal wetlands during growing season. Sci Total Environ 830:154460

Huang SH, Huang H, Zhu HY (2016) Effects of the addition of iron and aluminum salt on phosphorus adsorption in wetland sediment. Environ Sci Pollut Res 23:10022–10027

Huser BJ, Egemose S, Harper H, Hupfer M, Jensen H, Pilgrim KM, Reitzel K, Rydin E, Futter M (2016) Longevity and effectiveness of aluminum addition to reduce sediment phosphorus release and restore lake water quality. Water Res 97:122–132

Jeppesen E et al (2005) Lake responses to reduced nutrient loading - an analysis of contemporary long-term data from 35 case studies. Freshw Biol 50:1747–1771

Ji N, Liu Y, Wang S, Wu Z, Li H (2022) Buffering effect of suspended particulate matter on phosphorus cycling during transport from rivers to lakes. Water Res 216:118350

Jiao Y, Xu L, Li QM, Gu S (2020) Thin-layer fine-sand capping of polluted sediments decreases nutrients in overlying water of Wuhan Donghu Lake in China. Environ Sci Pollut Res 27:7156–7165

Kim LH, Choi E, Stenstrom MK (2003) Sediment characteristics, phosphorus types and phosphorus release rates between river and lake sediments. Chemosphere 50:53–61

Le Moal M, Gascuel-Odoux C, Ménesguen A, Souchon Y, Étrillard C, Levain A, Moatar F, Pannard A, Souchu P, Lefebvre A, Pinay G (2019) Eutrophication: a new wine in an old bottle? Sci Total Environ 651:1–11

Lei J, Lin J, Zhan Y, Zhang Z, Ma J (2021) Effectiveness and mechanism of aluminum/iron co-modified calcite capping and amendment for controlling phosphorus release from sediments. J Environ Manage 298:113471

Lei J, Lin J, Zhan Y, Wen X, Li Y (2022) Effect of sediment burial depth on the control of sedimentary phosphorus release by iron/aluminum co-modified calcite and strategy for overcoming the negative effect of sediment burial. Sci Total Environ 838:156467

Li QM, Shi WQ (2020) Effects of sediment oxidation on phosphorus transformation in three large shallow eutrophic lakes in China. Environ Sci Pollut Res 27:25925–25932

Li Y, Fan Y, Li X, Wu D (2017) Evaluation of zeolite/hydrous aluminum oxide as a sediment capping agent to reduce nutrients level in a pond. Ecol Eng 101:170–178

Li X, Xie Q, Chen S, Xing M, Guan T, Wu D (2019) Inactivation of phosphorus in the sediment of the Lake Taihu by lanthanum modified zeolite using laboratory studies. Environ Pollut 247:9–17

Li Y, Wang L, Yan Z, Chao C, Yu H, Yu D, Liu C (2020) Effectiveness of dredging on internal phosphorus loading in a typical aquacultural lake. Sci Total Environ 744:140883

Li Y, Wang L, Chao C, Yu H, Yu D, Liu C (2021) Submerged macrophytes successfully restored a subtropical aquacultural lake by controlling its internal phosphorus loading. Environ Pollut 268:115949

Li Y, Liu Y, Wang H, Zuo Z, Yan Z, Wang L, Wang D, Liu C, Yu D (2023) In situ remediation mechanism of internal nitrogen and phosphorus regeneration and release in shallow eutrophic lakes by combining multiple remediation techniques. Water Res 229:119394

Lin J, Sun Q, Ding SM, Wang D, Wang Y, Chen MS, Shi L, Fan XF, Tsang DCW (2017) Mobile phosphorus stratification in sediments by aluminum immobilization. Chemosphere 186:644–651

Lin J, He S, Zhan Y, Zhang Z, Wu X, Yu Y, Zhao Y, Wang Y (2019a) Assessment of sediment capping with zirconium-modified bentonite to intercept phosphorus release from sediments. Environ Sci Pollut Res 26:3501–3516

Lin J, He S, Zhang H, Zhan Y, Zhang Z (2019b) Effect of zirconium-modified zeolite addition on phosphorus mobilization in sediments. Sci Total Environ 646:144–157

Lin J, Wang Y, Zhan Y, Zhang Z (2019c) Magnetite-modified activated carbon based capping and mixing technology for sedimentary phosphorus release control. J Environ Manage 248:109287

Lin J, Zhao Y, Zhang Z, Zhan Y, Zhang Z, Wang Y, Yu Y, Wu X (2019d) Immobilization of mobile and bioavailable phosphorus in sediments using lanthanum hydroxide and magnetite/lanthanum hydroxide composite as amendments. Sci Total Environ 687:232–243

Lin J, Wang Y, He S, Zhan Y, Zhang Z, Wang D, Zhang Z (2020a) Synthesis and evaluation of zirconia/magnetite/zeolite composite for controlling phosphorus release from sediment: a laboratory study. Ecol Eng 151:105874

Lin JW, Wang Y, Zhan YH (2020b) Novel, recyclable active capping systems using fabric-wrapped zirconium-modified magnetite/bentonite composite for sedimentary phosphorus release control. Sci Total Environ 727:17

Liu C, Shao S, Shen Q, Fan C, Zhang L, Zhou Q (2016) Effects of riverine suspended particulate matter on the post-dredging increase in internal phosphorus loading across the sediment-water interface. Environ Pollut 211:165–172

Liu C, Du Y, Yin H, Fan C, Chen K, Zhong J, Gu X (2019) Exchanges of nitrogen and phosphorus across the sediment-water interface influenced by the external suspended particulate matter and the residual matter after dredging. Environ Pollut 246:207–216

Liu B, Liu Z, Yu P, Pan S, Xu Y, Sun Y, Pan S-Y, Yu Y, Zheng H (2020) Enhanced removal of tris(2-chloroethyl) phosphate using a resin-based nanocomposite hydrated iron oxide through a Fenton-like process: capacity evaluation and pathways. Water Res 175:115655

Liu B, Dai S, Zhang X, Cui F, Nan J, Wang W (2022) Highly efficient and reusable lanthanum-carbon nanotube films for enhanced phosphate removal. Sep Purif Technol 299:121710

Lu Z, Zhang K, Liu F, Gao X, Zhai Z, Li J, Du L (2022) Simultaneous recovery of ammonium and phosphate from aqueous solutions using Mg/Fe modified NaY zeolite: integration between adsorption and struvite precipitation. Sep Purif Technol 299:121713

Luo J, Peng C, Wang G, Qin L, Zheng J, Zhu X (2023) Selective removal of La(III) from mine tailwater using porous titanium phosphate monolith: adsorption behavior and mechanism. J Environ Chem Eng 11:109409

Mackay SE, Malherbe F, Eldridge DS (2022) Quaternary amine functionalized chitosan for enhanced adsorption of low concentration phosphate to remediate environmental eutrophication. Colloid Surface A 653:129984

Mallet M, Barthelemy K, Ruby C, Renard A, Naille S (2013) Investigation of phosphate adsorption onto ferrihydrite by X-ray photoelectron spectroscopy. J Colloid Interf Sci 407:95–101

Meis S, Spears BM, Maberly SC, O'Malley MB, Perkins RG (2012) Sediment amendment with Phoslock® in Clatto Reservoir (Dundee, UK): investigating changes in sediment elemental composition and phosphorus fractionation. J Environ Manag 93:185–193

Meis S, Spears BM, Maberly SC, Perkins RG (2013) Assessing the mode of action of Phoslock® in the control of phosphorus release from the bed sediments in a shallow lake (Loch Flemington, UK). Water Res 47:4460–4473

Min X, Wu X, Shao P, Ren Z, Ding L, Luo X (2019) Ultra-high capacity of lanthanum-doped UiO-66 for phosphate capture: unusual doping of lanthanum by the reduction of coordination number. Chem Eng J 358:321–330

Qu Y, Zhao L, Jin Z, Yang H, Tu C, Che F, Russel M, Song X, Huang W (2023) Study on the management efficiency of lanthanum/iron co-modified attapulgite on sediment phosphorus load. Chemosphere 313:137315

Ren Z, He J, Zhao H, Ding S, Duan P, Jiao L (2022) Water depth determines spatial and temporal phosphorus retention by controlling ecosystem transition and P-binding metal elements. Water Res 219:118550

Ribeiro DC, Martins G, Nogueira R, Cruz JV, Brito AG (2008) Phosphorus fractionation in volcanic lake sediments (Azores – Portugal). Chemosphere 70:1256–1263

Ross G, Haghseresht F, Cloete TE (2008) The effect of pH and anoxia on the performance of Phoslock®, a phosphorus binding clay. Harmful Algae 7:545–550

Rozemeijer J, Noordhuis R, Ouwerkerk K, Dionisio Pires M, Blauw A, Hooijboer A, van Oldenborgh GJ (2021) Climate variability effects on eutrophication of groundwater, lakes, rivers, and coastal waters in the Netherlands. Sci Total Environ 771:145366

Rydin E (2000) Potentially mobile phosphorus in Lake Erken sediment. Water Res 34:2037–2042

Schindler DW (1977) Evolution of phosphorus limitation in lakes. Science 195:260–262

Schindler DW, Carpenter SR, Chapra SC, Hecky RE, Orihel DM (2016) Reducing phosphorus to curb lake eutrophication is a success. Environ Sci Technol 50:8923–8929

Smith VH, Tilman GD, Nekola JC (1999) Eutrophication: impacts of excess nutrient inputs on freshwater, marine, and terrestrial ecosystems. Environ Pollut 100:179–196

Sondergaard M, Jensen JP, Jeppesen E (2003) Role of sediment and internal loading of phosphorus in shallow lakes. Hydrobiologia 506:135–145

Sun C, Wang S, Wang H, Hu X, Yang F, Tang M, Zhang M, Zhong J (2022) Internal nitrogen and phosphorus loading in a seasonally stratified reservoir: implications for eutrophication management of deep-water ecosystems. J Environ Manag 319:115681

Tang X, Li R, Han D, Wu X (2020) Impacts of electrokinetic isolation of phosphorus through pore water drainage on sediment phosphorus storage dynamics. Environ Pollut 266:115210

Tran HN, You S-J, Hosseini-Bandegharaei A, Chao H-P (2017) Mistakes and inconsistencies regarding adsorption of contaminants from aqueous solutions: a critical review. Water Res 120:88–116

Waajen G, van Oosterhout F, Douglas G, Lürling M (2016) Management of eutrophication in Lake De Kuil (The Netherlands) using combined flocculant – lanthanum modified bentonite treatment. Water Res 97:83–95

Walch H, von der Kammer F, Hofmann T (2022) Freshwater suspended particulate matter—key components and processes in floc formation and dynamics. Water Res 220:118655

Wang C, Liang J, Pei Y, Wendling LA (2013) A method for determining the treatment dosage of drinking water treatment residuals for effective phosphorus immobilization in sediments. Ecol Eng 60:421–427

Wang C, Yuan N, Pei Y, Jiang H-L (2015) Aging of aluminum/iron-based drinking water treatment residuals in lake water and their association with phosphorus immobilization capability. J Environ Manage 159:178–185

Wang Y, Ding SM, Wang D, Sun Q, Lin J, Shi L, Chen MS, Zhang CS (2017) Static layer: a key to immobilization of phosphorus in sediments amended with lanthanum modified bentonite (Phoslock®). Chem Eng J 325:49–58

Wang J, Chen J, Chen Q, Yang H, Zeng Y, Yu P, Jin Z (2019) Assessment on the effects of aluminum-modified clay in inactivating internal phosphorus in deep eutrophic reservoirs. Chemosphere 215:657–667

Wang Q, Liao Z, Yao D, Yang Z, Wu Y, Tang C (2021a) Phosphorus immobilization in water and sediment using iron-based materials: a review. Sci Total Environ 767:144246

Wang Y, Li J, Yuan Y, Si Y, Xu J, Li M, Peng X (2021b) $La(OH)_3$ loaded magnetic nanocomposites derived from sugarcane bagasse cellulose for phosphate adsorption: characterization, performance and mechanism. Colloid Surface A 626:127060

Wang X, Zhi Y, Chen Y, Shen N, Wang G, Yan Y (2022) Realignment of phosphorus in lake sediment induced by sediment microbial fuel cells (SMFC). Chemosphere 291:132927

Wang Y, Peng Z, Liu G, Zhang H, Zhou X, Hu W (2023) A mathematical model for phosphorus interactions and transport at the sediment-water interface in a large shallow lake. Ecol Model 476:110254

Wen S, Zhong J, Li X, Liu C, Yin H, Li D, Ding S, Fan C (2020) Does external phosphorus loading diminish the effect of sediment dredging on internal phosphorus loading? An in-situ simulation study. J Hazard Mater 394:122548

Wu X, Ma T, Du Y, Jiang Q, Shen S, Liu W (2021) Phosphorus cycling in freshwater lake sediments: influence of seasonal water level fluctuations. Sci Total Environ 792:148383

Wu D, Zhan Y, Lin J, Zhang Z, Xie B (2022a) Contrasting effect of lanthanum hydroxide and lanthanum carbonate treatments on phosphorus mobilization in sediment. Chem Eng J 427:132021

Wu Y, Song L, Shi M, Gu C, Zhang J, Lv J, Xuan L (2022b) Ca/Fe-layered double hydroxide–zeolite composites for the control of phosphorus pollution in sediments: performance, mechanisms, and microbial community response. Chem Eng J 450:138277

Xia L, David T, Verbeeck M, Bruneel Y, Smolders E (2022) Iron rich glauconite sand as an efficient phosphate immobilising agent in river sediments. Sci Total Environ 811:152483

Xia L, van Dael T, Bergen B, Smolders E (2023) Phosphorus immobilisation in sediment by using iron rich by-product as affected by water pH and sulphate concentrations. Sci Total Environ 864:160820

Yamada TM, Sueitt AP, Beraldo DA, Botta CM, Fadini PS, Nascimento MR, Faria BM, Mozeto AA (2012) Calcium nitrate addition to control the internal load of phosphorus from sediments of a tropical eutrophic reservoir: microcosm experiments. Water Res 46:6463–6475

Yan Z, Wu L, Lv T, Tong C, Gao Z, Liu Y, Xing B, Chao C, Li Y, Wang L, Liu C, Yu D (2022) Response of spatio-temporal changes in sediment phosphorus fractions to vegetation restoration in the degraded river-lake ecotone. Environ Pollut 308:119650

Yang MJ, Lin JW, Zhan YH, Zhu ZL, Zhang HH (2015) Immobilization of phosphorus from water and sediment using zirconium-modified zeolites. Environ Sci Pollut Res 22:3606–3619

Yang C, Yang P, Geng J, Yin H, Chen K (2020a) Sediment internal nutrient loading in the most polluted area of a shallow eutrophic lake (Lake Chaohu, China) and its contribution to lake eutrophication. Environ Pollut 262:114292

Yang P, Yang C, Yin H (2020b) Dynamics of phosphorus composition in suspended particulate matter from a turbid eutrophic shallow lake (Lake Chaohu, China): implications for phosphorus cycling and management. Sci Total Environ 741:140203

Yang C, Wang G, Yin H (2023) Response of internal phosphorus loading from dredged and inactivated sediment under repeated resuspension in a eutrophic shallow lake. Sci Total Environ 868:161653

Yasseri S, Epe TS (2016) Analysis of the La: P ratio in lake sediments – vertical and spatial distribution assessed by a multiple-core survey. Water Res 97:96–100

Yin HB, Han MX, Tang WY (2016) Phosphorus sorption and supply from eutrophic lake sediment amended with thermally-treated calcium-rich attapulgite and a safety evaluation. Chem Eng J 285:671–678

Yin H, Du Y, Kong M, Liu C (2017) Interactions of riverine suspended particulate matter with phosphorus inactivation agents across sediment-water interface and the implications for eutrophic lake restoration. Chem Eng J 327:150–161

Yin H, Douglas GB, Cai Y, Liu C, Copetti D (2018a) Remediation of internal phosphorus loads with modified clays, influence of fluvial suspended particulate matter and response of the benthic macroinvertebrate community. Sci Total Environ 610–611:101–110

Yin H, Ren C, Li W (2018b) Introducing hydrate aluminum into porous thermally-treated calcium-rich attapulgite to enhance its phosphorus sorption capacity for sediment internal loading management. Chem Eng J 348:704–712

Yin HB, Zhu JC, Tang WY (2018c) Management of nitrogen and phosphorus internal loading from polluted river sediment using Phoslock® and modified zeolite with intensive tubificid oligochaetes bioturbation. Chem Eng J 353:46–55

Yin H, Yang P, Kong M, Li W (2020) Use of lanthanum/aluminum co-modified granulated attapulgite clay as a novel phosphorus (P) sorbent to immobilize P and stabilize surface sediment in shallow eutrophic lakes. Chem Eng J 385:123395

Yin H, Yang C, Yang P, Kaksonen AH, Douglas GB (2021) Contrasting effects and mode of dredging and in situ adsorbent amendment for the control of sediment internal phosphorus loading in eutrophic lakes. Water Res 189:116644

Yin H, Zhang M, Yin P, Li J (2022) Characterization of internal phosphorus loading in the sediment of a large eutrophic lake (Lake Taihu, China). Water Res 225:119125

Yu J, Ding S, Zhong J, Fan C, Chen Q, Yin H, Zhang L, Zhang Y (2017) Evaluation of simulated dredging to control internal phosphorus release from sediments: focused on phosphorus transfer and resupply across the sediment-water interface. Sci Total Environ 592:662–673

Yu J, Zeng Y, Chen J, Liao P, Yang H, Yin C (2022) Organic phosphorus regeneration enhanced since eutrophication occurred in the sub-deep reservoir. Environ Pollut 306:119350

Yuan L, Qiu Z, Lu Y, Tariq M, Yuan L, Yang J, Li Z, Lyu S (2018) Development of lanthanum hydroxide loaded on molecular sieve adsorbent and mechanistic study for phosphate removal. J Alloy Compd 768:953–961

Yuan H, Tai Z, Li Q, Liu E (2020) In-situ, high-resolution evidence from water-sediment interface for significant role of iron bound phosphorus in eutrophic lake. Sci Total Environ 706:136040

Yuan M, Qiu S, Li M, Di Z, Feng M, Guo C, Fu W, Zhang K, Hu W, Wang F (2023) Enhancing phosphate removal performance in water using La–Ca/Fe–LDH: La loading alleviates ineffective stacking of laminates and increases the number of active adsorption sites. J Clean Prod 388:135857

Zeller MA, Alperin MJ (2021) The efficacy of Phoslock® in reducing internal phosphate loading varies with bottom water oxygenation. Water Res X 11:100095

Zhan Y, Yu Y, Lin J, Wu X, Wang Y, Zhao Y (2019) Simultaneous control of nitrogen and phosphorus release from sediments using iron-modified zeolite as capping and amendment materials. J Environ Manage 249:109369

Zhang X, Liu M, Han R (2021) Adsorption of phosphate on UiO-66-NH2 prepared by a green synthesis method. J Environ Chem Eng 9:106672

Zhang B, Xu L, Zhao Z, Peng S, Yu C, Zhang X, Zong Y, Wu D (2022) Enhanced phosphate removal by nano-lanthanum hydroxide embedded silica aerogel composites: superior performance and insights into specific adsorption mechanism. Sep Purif Technol 285:120365

Zhang F, Yan J, Fang J, Yan Y, Zhang S, Benoit G (2023) Sediment phosphorus immobilization with the addition of calcium/aluminum and lanthanum/calcium/aluminum composite materials under wide ranges of pH and redox conditions. Sci Total Environ 863:160997

Zhou J, Li D, Chen S, Xu Y, Geng X, Guo C, Huang Y (2019) Sedimentary phosphorus immobilization with the addition of amended calcium peroxide material. Chem Eng J 357:288–297

Zhou J, Leavitt PR, Zhang Y, Qin B (2022) Anthropogenic eutrophication of shallow lakes: is it occasional? Water Res 221:118728

Zyoud AH, Zubi A, Zyoud SH, Hilal MH, Zyoud S, Qamhieh N, Hajamohideen A, Hilal HS (2019) Kaolin-supported ZnO nanoparticle catalysts in self-sensitized tetracycline photodegradation: zero-point charge and pH effects. Appl Clay Sci 182:105294